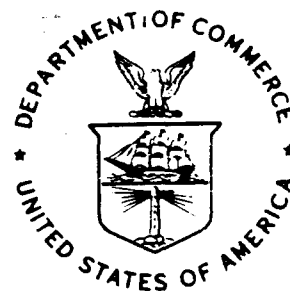NOAA Technical Memorandum NWS WR-196

A MESOSCALE CONVECTIVE COMPLEX TYPE STORM OVER THE DESERT SOUTHWEST

Salt Lake City, Utah
April 1986

NOAA TECHNICAL MEMORANDA
National Weather Service, Western Region Subseries

The National Weather Service (NWS) Western Region (WR) Subseries provides an informal medium for the documentation and quick dissemination of results not appropriate, or not yet ready, for formal publication. The series is used to report on work in progress, to describe technical procedures and practices, or to relate progress to a limited audience. These Technical Memoranda will report on investigations devoted primarily to regional and local problems of interest mainly to personnel, and hence will not be widely distributed.

Papers 1 to 25 are in the former series, ESSA Technical Memoranca, Western Region Technical Memoranda (WRTM); papers 24 to 59 are in the former series, ESSA Technical Memoranda, Weather Bureau Technical Memoranda (WBTM). Beginning with 60, the papers are part of the series, NOAA Technical Memorada NWS. Out-of-print memoranda are not listed.

Papers 2 to 22, except for 5 (revised edition), are available from the National Weather Service Western Region, Scientific Services Division, P. O. Box 11188, Federal Building, 125 South State Street, Salt Lake City. Utah 84147. Paper 5 (revised edition), and all others beginning with 25 are available from the National Technical Information Service, U. S. Department of Commerce, Sills Building, 5285 Port Royal Road, Springfield, Virginia 22161 Prices vary for all paper copy; $3.50 microfiche. Order by accession number shown in parentheses at end of each entry.

ESSA Technical Memoranda (WRTM)

2   Climatological Precipitation Probabilities. Compiled by Lucianne Miller, December 1965.
3   Western Region Pre- and Post-FP-3 Program, December 1, 1965, to February 20, 1966. Edward D. Diemer, March 1966.
5   Station Descriptions of Local Effects on Synoptic Weather Patterns. Philip Williams, Jr., April 1966 (revised November 1967, October 1969). (PB-17800)
8   Interpreting the RAREP. Herbert P. Benner, May 1966 (revised January 1967).
11  Some Electrical Processes in the Atmosphere. J. Latham, June 1966.
17  A Digitalized Summary of Radar Echoes within 100 Miles of Sacramento, California. J. A. Youngberg and L. B. Overaas, December 1966.
21  An Objective Aid for Forecasting the End of East Winds in the Columbia Gorge, July through October. D. John Coparanis, April 1967.
22  Derivation of Radar Horizons in Mountainous Terrain. Roger G. Pappas, April 1967.

ESSA Technical Memoranda, Weather Bureau Technical Memoranda (WBTM)

25  Verification of Operational Probability of Precipitation Forecasts, April 1966-March 1967. W. W. Dickey, October 1967. (PB-176240)
26  A Study of Winds in the Lake Mead Recreation Area. R. P. Augulis. January 1968. (PB-177830)
28  Weather Extremes. R. J. Schmidli, April 1968 (Revised March 1986). (PB178425)
29  Small-Scale Analysis and Prediction. Philip Williams, Jr., May 1968. (PB178425)
30  Numerical Weather Prediction and Synoptic Meteorology. Capt. Thomas D. Murphy, U.S.A.F., May 1968. (AD-673365)
31  Precipitation Detection Probabilities by Salt Lake ARTC Radars. Robert K. Belesky, July 1968. (PB-179084)
32  Probability Forecasting--A Problem Analysis with Reference to the Portland Fire Weather District. Harold S. Ayer, July 1968. (PB-179289)
35  Joint ESSA/FAA ARTC Radar Weather Surveillance Program. Herbert P. Benner and DeVon B. Smith, December 1968 (revised June 1970). AD-681857)
36  Temperature Trends in Sacramento--Another Heat Island. Anthony D. Lentini, February 1969. (PB-183055)
37  Disposal of Logging Residues without Damage to Air Quality. Owen P. Cramer, March 1969. (PB-183057)
39  Upper-Air Lows over Northwestern United States. A. L. Jacobson, April 1969. (PB-184296)
40  The Man-Machine Mix in Applied Weather Forecasting in the 1970's. L. W. Snellman, August 1969. (PB-185068)
42  Analysis of the Southern California Santa Ana of January 15-17, 1966. Barry B. Aronovitch, August 1969. (PB-185670)
43  Forecasting Maximum Temperatures at Helena, Montana. David E. Olsen, October 1969. (PB-185762)
44  Estimated Return Periods for Short-Duration Precipitation in Arizona. Paul C. Kangieser, October 1969. (PB-187763)
46  Applications of the Net Radiometer to Short-Range Fog and Stratus Forecasting at Eugene, Oregon. L. Yee and E. Bates, December 1969. (PB-190476)
47  Statistical Analysis as a Flood Routing Tool. Robert J. C. Burnash, December 1969. (PB-188744)
48  Tsunami. Richard P. Augulis, February 1970. (PB-190157)
49  Predicting Precipitation Type. Robert J. C. Burnash and Floyd E. Hug, March 1970. (PB-190962)
50  Statistical Report on Aeroallergens (Pollens and Molds) Fort Huachuca, Arizona, 1969. Wayne S. Johnson, April 1970. (PB-191743)
51  Western Region Sea State and Surf Forecaster's Manual. Gordon C. Shields and Gerald B. Burdwell, July 1970. (PB-193102)
52  Sacramento Weather Radar Climatology. R. G. Pappas and C. M. Veliquette, July 1970. (PB-193347)
54  A Refinement of the Vorticity Field to Delineate Areas of Significant Precipitation. Barry B. Aronovitch, August 1970.
55  Application of the SSARR Model to a Basin without Discharge Record. Vail Schermerhorn and Donal W. Kuehl, August 1970. (PB-194394)
56  Areal Coverage of Precipitation in Northwestern Utah. Philip Williams, Jr., and Werner J. Heck, September 1970. (PB-194389)
57  Preliminary Report on Agricultural Field Burning vs. Atmospheric Visibility in the Willamette Valley of Oregon. Earl M. Bates and David O. Chilcote, September 1970. (PB-194710)
58  Air Pollution by Jet Aircraft at Seattle-Tacoma Airport. Wallace R. Donaldson, October 1970. (COM-71-00017)
59  Application of PE Model Forecast Parameters to Local-Area Forecasting. Leonard W. Snellman, October 1970. (COM-71-00016)

NOAA Technical Memoranda (NWS WR)

60  An Aid for Forecasting the Minimum Temperature at Medford, Oregon. Arthur W. Fritz, October 1970. (COM-71-00120)
63  700-mb Warm Air Advection as a Forecasting Tool for Montana and Northern Idaho. Norris E. Woerner, February 1971. (COM-71-00349)
64  Wind and Weather Regimes at Great Falls, Montana. Warren B. Price, March 1971.
66  A Preliminary Report on Correlation of ARTCC Radar Echoes and Precipitation. Wilbur K. Hall, June 1971. (COM-71-00829)
69  National Weather Service Support to Soaring Activities. Ellis Burton, August 1971. (COM-71-00956)
71  Western Region Synoptic Analysis-Problems and Methods. Philip Williams, Jr., February 1972. (COM-72-10433)
74  Thunderstorms and Hail Days Probabilities in Nevada. Clarence M. Sakamoto, April 1972. (COM-72-10554)
75  A Study of the Low Level Jet Stream of the San Joaquin Valley. Ronald A. Willis and Philip Williams, Jr., May 1972. (COM-72-10707)
76  Monthly Climatological Charts of the Behavior of Fog and Low Stratus at Los Angeles International Airport. Donald M. Gales, July 1972. (COM-72-11140)
77  A Study of Radar Echo Distribution in Arizona During July and August. John E. Hales, Jr., July 1972. (COM-72-11136)
78  Forecasting Precipitation at Bakersfield, California, Using Pressure Gradient Vectors. Earl T. Riddiough, July 1972. (COM-72-11146)
79  Climate of Stockton, California. Robert C. Nelson, July 1972. (COM-72-10920)
80  Estimation of Number of Days Above or Below Selected Temperatures. Clarence M. Sakamoto, October 1972. (COM-72-10021)
81  An Aid for Forecasting Summer Maximum Temperatures at Seattle, Washington. Edgar G. Johnson, November 1972. (COM-73-10150)
82  Flash Flood Forecasting and Warning Program in the Western Region. Philip Williams, Jr., Chester L. Glenn, and Roland L. Raetz, December 1972, (revised March 1978). (COM-73-10251)
83  A Comparison of Manual and Semiautomatic Methods of Digitizing Analog Wind Records. Glenn E. Rasch, March 1973. (COM-73-10669)
86  Conditional Probabilities for Sequences of Wet Days at Phoenix, Arizona. Paul C. Kangieser, June 1973. (COM-73-11264)
87  A Refinement of the Use of K-Values in Forecasting Thunderstorms in Washington and Oregon. Robert Y. G. Lee, June 1973. (COM-73-11276)
89  Objective Forecast Precipitation over the Western Region of the United States. Julia N. Paegle and Larry P. Kierulff, Sept. 1973. (COM-73-11946/3AS)
91  Arizona "Eddy" Tornadoes. Robert S. Ingram, October 1973. (COM-73-10465)
92  Smoke Management in the Willamette Valley. Earl M. Bates, May 1974. (COM-74-11277/AS)
93  An Operational Evaluation of 500-mb Type Regression Equations. Alexander E. MacDonald, June 1974. (COM-74-11407/AS)
94  Conditional Probability of Visibility Less than One-Half Mile in Radiation Fog at Fresno, California. John D. Thomas, August 1974. (COM-74-11555/AS)
96  Map Type Precipitation Probabilities for the Western Region. Glenn E. Rasch and Alexander E. MacDonald, February 1975. (COM-75-10428/AS)
97  Eastern Pacific Cut-Off Low of April 21-28, 1974. William J. Alder and George R. Miller, January 1976. (PB-250-711/AS)
98  Study on a Significant Precipitation Episode in Western United States. Ira S. Brenner, April 1976. (COM-75-10719/AS)
99  A Study of Flash Flood Susceptibility--A Basin in Southern Arizona. Gerald Williams, August 1975. (COM-75-11360/AS)
102 A Set of Rules for Forecasting Temperatures in Napa and Sonoma Counties. Wesley L. Tuft, October 1975. (PB-246-902/AS)
103 Application of the National Weather Service Flash-Flood Program in the Western Region. Gerald Williams, January 1976. (PB-253-053/AS)
104 Objective Aids for Forecasting Minimum Temperatures at Reno, Nevada, During the Summer Months. Christopher D. Hill, January 1976. (PB-252-866/AS)
105 Forecasting the Mono Wind. Charles P. Ruscha, Jr., February 1976. (PB-254-650)
106 Use of MOS Forecast Parameters in Temperature Forecasting. John C. Plankinton, Jr., March 1976. (PB-254-649)
107 Map Types as Aids in Using MOS PoPs in Western United States. Ira S. Brenner, August 1976. (PB-259-594)
108 Other Kinds of Wind Shear. Christopher D. Hill, August 1976. (PB-260-437/AS)
109 Forecasting North Winds in the Upper Sacramento Valley and Adjoining Forests. Christopher E. Fontana, September 1976. (PB-273-677/AS)
110 Cool Inflow as a Weakening Influence on Eastern Pacific Tropical Cyclones. William J. Denney, November 1976. (PB-264-655/AS)
112 The MAN/MOS Program. Alexander E. MacDonald, February 1977. (PB-265-941/AS)
113 Winter Season Minimum Temperature Formula for Bakersfield, California, Using Multiple Regression. Michael J. Oard, February 1977. (PB-273-694/AS)
114 Tropical Cyclone Kathleen. James R. Fors, February 1977. (PB-273-676/AS)
116 A Study of Wind Gusts on Lake Mead. Bradley Colman, April 1977. (PB-268-847)
117 The Relative Frequency of Cumulonimbus Clouds at the Nevada Test Site as a Function of K-Value. R. F. Quiring, April 1977. (PB-272-831)
118 Moisture Distribution Modification by Upward Vertical Motion. Ira S. Brenner, April 1977. (PB-268-740)
119 Relative Frequency of Occurrence of Warm Season Echo Activity as a Function of Stability Indices Computed from the Yucca Flat, Nevada, Rawinsonde. Darryl Randerson, June 1977. (PB-271-290/AS)

121 Climatological Prediction of Cumulonimbus Clouds in the Vicinity of the Yucca Flat Weather Station. R. F. Quiring, June 1977. (PB-271-704/AS)
122 A Method for Transforming Temperature Distribution to Normality. Morris S. Webb, Jr., June 1977. (PB-271-742/AS)
124 Statistical Guidance for Prediction of Eastern North Pacific Tropical Cyclone Motion - Part I. Charles J. Neumann and Preston W. Leftwich, August 1977. (PB-272-661)
125 Statistical Guidance on the Prediction of Eastern North Pacific Tropical Cyclone Motion - Part II. Preston W. Leftwich and Charles J. Neumann, August 1977. (PB-273-155/AS)
127 Development of a Probability Equation for Winter-Type Precipitation Patterns in Great Falls, Montana. Kenneth B. Mielke, February 1978.(PB-281-387/AS)
128 Hand Calculator Program to Compute Parcel Thermal Dynamics. Dan Gudgel, April 1978. (PB-283-080/AS)
129 Fire Whirls. David W. Goens, May 1978. (PB-283-866/AS)
130 Flash-Flood Procedure. Ralph C. Hatch and Gerald Williams, May 1978. (PB-286-014/AS)
131 Automated Fire-Weather Forecasts. Mark A. Mollner and David E. Olsen, September 1978. (PB-289-916/AS)
132 Estimates of the Effects of Terrain Blocking on the Los Angeles WSR-74C Weather Radar. R. G. Pappas, R. Y. Lee, B. W. Finke, October 1978.(PB289767/AS)
133 Spectral Techniques in Ocean Wave Forecasting. John A. Jannuzzi, October 1978. (PB291317/AS)
134 Solar Radiation. John A. Jannuzzi, November 1978. (PB291195/AS)
135 Application of a Spectrum Analyzer in Forecasting Ocean Swell in Southern California Coastal Waters. Lawrence P. Kierulff, January 1979. (PB292716/AS)
136 Basic Hydrologic Principles. Thomas L. Dietrich, January 1979. (PB292247/AS)
137 LFM 24-Hour Prediction of Eastern.Pacific Cyclones Refined by Satellite Images. John R. Zimmerman and Charles P. Ruscha, Jr., Jan. 1979. (PB294324/AS)
138 A Simple Analysis/Diagnosis System for Real Time Evaluation of Vertical Motion. Scott Heflick and James R. Fors, February 1979. (PB294216/AS)
139 Aids for Forecasting Minimum Temperature in the Wenatchee Frost District. Robert S. Robinson, April 1979. (PB298339/AS)
140 Influence of Cloudiness on Summertime Temperatures in the Eastern Washington Fire Weather District. James Holcomb, April 1979. (PB298674/AS)
141 Comparison of LFM and MFM Precipitation Guidance for Nevada During Doreen. Christopher Hill, April 1979. (PB298613/AS)
142 The Usefulness of Data from Mountaintop Fire Lookout Stations in Determining Atmospheric Stability. Jonathan W. Corey, April 1979. (PB298899/AS)
143 The Depth of the Marine Layer at San Diego as Related to Subsequent Cool Season Precipitation Episodes in Arizona. Ira S. Brenner, May 1979. (PB298817/AS)
144 Arizona Cool Season Climatological Surface Wind and Pressure Gradient Study. Ira S. Brenner, May 1979. (PB298900/AS)
145 On the Use of Solar Radiation and Temperature Models to Estimate the Snap Bean Maturity Date in the Willamette Valley. Earl M. Bates, August 1979. (PB80-160971)
146 The BART Experiment. Morris S. Webb, October 1979. (PB80-155112)
147 Occurrence and Distribution of Flash Floods in the Western Region. Thomas L. Dietrich, December 1979. (PB80-160344)
149 Misinterpretations of Precipitation Probability Forecasts. Allan H. Murphy, Sarah Lichtenstein, Baruch Fischhoff, and Robert L. Winkler, February 1980. (PB80-174576)
150 Annual Data and Verification Tabulation - Eastern and Central North Pacific Tropical Storms and Hurricanes 1979. Emil B. Gunther and Staff, EPHC, April 1980. (PB80-220486)
151 NMC Model Performance in the Northeast Pacific. James E. Overland, PMEL-ERL, April 1980. (PB80-196033)
152 Climate of Salt Lake City, Utah. Wilbur E. Figgins, October 1984. 2nd Revision. (PB85 123875)
153 An Automatic Lightning Detection System in Northern California. James E. Rea and Chris E. Fontana, June 1980. (PB80-225592)
154 Regression Equation for the Peak Wind Gust 6 to 12 Hours in Advance at Great Falls During Strong Downslope Wind Storms. Michael J. Oard, July 1980. (PB81-108367)
155 A Raininess Index for the Arizona Monsoon. John H. TenHarkel, July 1980. (PB81-106494)
156 The Effects of Terrain Distribution on Summer Thunderstorm Activity at Reno, Nevada. Christopher Dean Hill, July 1980. (PB81-102501)
157 An Operational Evaluation of the Scofield/Oliver Technique for Estimating Precipitation Rates from Satellite Imagery. Richard Ochoa, August 1980. (PB81-108227)
158 Hydrology Practicum. Thomas Dietrich, September 1980. (PB81-134033)
159 Tropical Cyclone Effects on California. Arnold Court, October 1980. (PB81-133779)
160 Eastern North Pacific Tropical Cyclone Occurrences During Intraseasonal Periods. Preston W. Leftwich and Gail M. Brown, February 1981. (PB81-205494)
161 Solar Radiation as a Sole Source of Energy for Photovoltaics in Las Vegas, Nevada, for July and December. Darryl Randerson, April 1981. (PB81-224503)
162 A Systems Approach to Real-Time Runoff Analysis with a Deterministic Rainfall-Runoff Model. Robert J. C. Burnash and R. Larry Ferral, April 1981. (PB81-224495)
163 A Comparison of Two Methods for Forecasting Thunderstorms at Luke Air Force Base, Arizona. Lt. Colonel Keith R. Cooley, April 1981. (PB81-225393)
164 An Objective Aid for Forecasting Afternoon Relative Humidity Along the Washington Cascade East Slopes. Robert S. Robinson, April 1981. (PB81-23678)
165 Annual Data and Verification Tabulation, Eastern North Pacific Tropical Storms and Hurricanes 1980. Emil B. Gunther and Staff, May 1981. (PB82-230336)
166 Preliminary Estimates of Wind Power Potential at the Nevada Test Site. Howard G. Booth, June 1981. (PB82-127036)
167 ARAP User's Guide. Mark Mathewson, July 1981. (revised September 1981). (PB82-196783)
168 Forecasting the Onset of Coastal Gales Off Washington-Oregon. John R. Zimmerman and William D. Burton, August 1981. (PB82-127051)
169 A Statistical-Dynamical Model for Prediction of Tropical Cyclone Motion in the Eastern North Pacific Ocean. Preston W. Leftwich, Jr., October 1981.
170 An Enhanced Plotter for Surface Airways Observations. Andrew J. Spry and Jeffrey L. Anderson, October 1981. (PB82-153883)
171 Verification of 72-Hour 500-mb Map-Type Predictions. R. F. Quiring, November 1981. (PB82-158098)
172 Forecasting Heavy Snow at Wenatchee, Washington. James W. Holcomb, December 1981. (PB82-177783)
173 Central San Joaquin Valley Type Maps. Thomas R. Crossan, December 1981. (PB82-196064)
174 ARAP Test Results. Mark A. Mathewson, December 1981. (PB82-193103)
175 Annual Data and Verification Tabulation Eastern North Pacific Tropical Storms and Hurricanes 1981. Emil B. Gunther and Staff, June 1982.(PB82-252420)
176 Approximations to the Peak Surface Wind Gusts from Desert Thunderstorms. Darryl Randerson, June 1982. (PB82-253089)
177 Climate of Phoenix, Arizona. Robert J. Schmidli, April 1969 (revised March 1983). (PB83246801)
178 Annual Data and Verification Tabulation, Eastern North Pacific Tropical Storms and Hurricanes 1982. E. B. Gunther, June 1983. (PB85 106078)
179 Stratified Maximum Temperature Relationships Between Sixteen Zone Stations in Arizona and Respective Key Stations. Ira S. Brenner, June 1983. (PB83-249904)
180 Standard Hydrologic Exchange Format (SHEF) Version I. Phillip A. Pasteries, Vernon C. Bissel, David G. Bennett, August, 1983.(PB85 106052)
181 Quantitative and Spacial Distribution of Winter Precipitation Along Utah's Wasatch Front. Lawrence B. Dunn, August, 1983. (PB85 106912)
182 500 Millibar Sign Frequency Teleconnection Charts - Winter. Lawrence B. Dunn, December, 1983.
183 500 Millibar Sign Frequency Teleconnection Charts - Spring. Lawrence B. Dunn, January, 1984. (PB85 111367)
184 Collection and Use of Lightning Strike Data in the Western U.S. During Summer 1983. Glenn Rasch and Mark Mathewson, February, 1984. (PB85 115559)
185 500 Millibar Sign Frequency Teleconnection Charts - Summer. Lawrence B. Dunn, March 1984. (PB85 111359)
186 Annual Data and Verification Tabulation Eastern North Pacific Tropical Storms and Hurricanes 1983. E. B. Gunther, March 1984. (PB85 109635)
187 500 Millibar Sign Frequency Teleconnection Charts - Fall. Lawrence B. Dunn, May 1984. (PB85 110930)
188 The Use and Interpretation of Isentropic Analyses. Jeffrey L. Anderson, October 1984. (PB85 132694)
189 Annual Data & Verification Tabulation Eastern North Pacific Tropical Storms and Hurricanes 1984. E. B. Gunther and R. L. Cross, April 1985. (PB85 187888PAS)
190 Great Salt Lake Effect Snowfall: Some Notes and An Example. David M. Carpenter, October 1985.
191 Large Scale Patterns Associated with Major Freeze Episodes in the Agricultural Southwest. Ronald S. Hamilton and Glenn R. Lussky, December 1985.
192 NWR Voice Synthesis Project: Phase I. Glen W. Sampson, January 1986.
193 The MCC - An Overview and Case Study on Its Impact in the Western United States. Glenn R. Lussky, March 1986.
194 Annual Data and Verification Tabulation Eastern North Pacific Tropical Storms and Hurricanes 1985. E. B. Gunther and R. L. Cross, March 1986.
195 Radid Interpretation Guidelines. Roger G. Pappas, March 1986.

# NOAA SCIENTIFIC AND TECHNICAL PUBLICATIONS

*The National Oceanic and Atmospheric Administration* was established as part of the Department of Commerce on October 3, 1970. The mission responsibilities of NOAA are to assess the socioeconomic impact of natural and technological changes in the environment and to monitor and predict the state of the solid Earth, the oceans and their living resources, the atmosphere, and the space environment of the Earth.

The major components of NOAA regularly produce various types of scientific and technical information in the following kinds of publications:

PROFESSIONAL PAPERS — Important definitive research results, major techniques, and special investigations.

CONTRACT AND GRANT REPORTS — Reports prepared by contractors or grantees under NOAA sponsorship.

ATLAS — Presentation of analyzed data generally in the form of maps showing distribution of rainfall, chemical and physical conditions of oceans and atmosphere, distribution of fishes and marine mammals, ionospheric conditions, etc.

TECHNICAL SERVICE PUBLICATIONS — Reports containing data, observations, instructions, etc. A partial listing includes data serials; prediction and outlook periodicals; technical manuals, training papers, planning reports, and information serials; and miscellaneous technical publications.

TECHNICAL REPORTS — Journal quality with extensive details, mathematical developments, or data listings.

TECHNICAL MEMORANDUMS — Reports of preliminary, partial, or negative research or technology results, interim instructions, and the like.



*Information on availability of NOAA publications can be obtained from:*

**ENVIRONMENTAL SCIENCE INFORMATION CENTER (D822)**
**ENVIRONMENTAL DATA AND INFORMATION SERVICE**
**NATIONAL OCEANIC AND ATMOSPHERIC ADMINISTRATION**
**U.S. DEPARTMENT OF COMMERCE**

**6009 Executive Boulevard**
**Rockville, MD 20852**

NOAA Technical Memorandum NWS WR-196

A MESOSCALE CONVECTIVE COMPLEX TYPE STORM OVER THE DESERT SOUTHWEST

Darryl Randerson

Nuclear Support Office
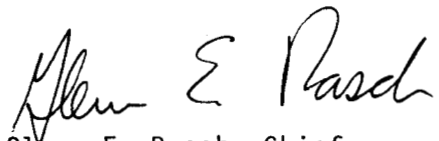National Weather Service
Las Vegas, Nevada
April 1986

This publication has been reviewed

and is approved for publication by

Scientific Services Division,

Western Region.

Glenn E. Rasch, Chief
Scientific Services Division
Western Region Headquarters
Salt Lake City, Utah

TABLE OF CONTENTS

FIGURES

## TABLES

# A MESOSCALE CONVECTIVE COMPLEX TYPE
## STORM OVER THE DESERT SOUTHWEST

Darryl Randerson
Nuclear Support Office
National Weather Service

ABSTRACT. On 10 August 1981 a mesoscale convective complex (MCC) developed over extreme east-central Nevada and moved south-southeastward into northwestern Arizona. This storm affected a total area of nearly 200,000 km$^2$, traveled approximately 500 km, and lasted nearly 15 hr. Strong surface winds, hail, heavy rain, and dense blowing dust and sand were reported on the right flank of the MCC. Estimated rainfall rates of 3 to 4 in/hr produced total rainfall amounts of 3 to 6 in over a large area to the northeast of Las Vegas, Nevada. Integration of the isohyetal analysis showed that approximately 10$^9$m$^3$ (8 X 10$^5$ acre ft) of water was available before infiltration. In terms of the volume of rain water produced, this storm was 30 times larger than the one that struck Las Vegas, Nevada, on 3 July, 1975. Severe flooding occurred, causing much property damage and loss of livestock in the Logandale/Glendale, Nevada, area. The MCC developed ahead of a southward moving short wave trough as the trough moved into an area of unstable moist air. MCC generation may have been enhanced by the presence of a developing east-west moisture gradient and by intense surface heating. The heavy weather produced by the MCC was closely related to very cold (-65°C) cloud-top temperatures and to strong surface convergence.

## I. INTRODUCTION

A. Overview

Large cumulonimbus can develop over the desert southwest during the summertime. These storms can be accompanied by locally heavy rain, strong surface winds, and hail. Over desert areas, strong outflow winds from thunderstorms frequently cause dense blowing dust and/or sand that may limit horizontal visibility to less than 1 mile. Idso et al. (1972) reported that dust clouds generated by desert thunderstorms have been observed to extend upward to near the 8,000-foot level above sea level. Such conditions are not only hazardous to aircraft operations but also to vehicles traveling on the ground. These storms can produce and maintain mesoscale surface high (and low) pressure systems. Consequently, except for blowing dust, the surface weather features accompanying these storms are quite similar to those of severe thunderstorms commonly associated with the midwestern states.

Intense thunderstorms are not uncommon in the desert southwest and northwestern Mexico during the summer. Occurrences of intense desert thunderstorms have been documented by Blake (1923), Reed (1937), Bailey (1966), Hales (1975), Randerson (1976a), and others. Some of these thunderstorms appear to organize into mesoscale storm systems with cold ( ≤-52°C) cloud tops and long duration times ( ≥6 hr). Convectively driven weather systems of this type have

been identified over the central United States by Maddox (1980). Indeed, this type of weather system is so important it has been named Mesoscale Convective Complex or MCC (e.g., see Maddox, 1980). Little effort has been expended to determine if MCC's occur over the western United States. Limited data point to the formation of MCC's over the desert southwest in July through September. The storm of 10 August 1981 appears to satisfy most of the physical characteristics of an MCC.

B. The Thunderstorm

In the early afternoon of 10 August 1981, thunderstorm activity over east central Nevada started to organize into one large cloud mass. This development can be seen in the infrared satellite imagery in Figures 1 and 2. For 4 hr (1946 to 2346Z or 1146 to 1546 PST) the cloud mass continued to consolidate and grow in areal extent as cloud-top temperatures cooled. Based on these two characteristics, the southeastwardly moving storm system reached its maximum intensity between 0000Z and 0400Z on 11 August (1600 and 2000 PST, 10 August). As the storm moved southeastward into central Arizona, it slowly dissipated, turned eastward, and became indistinguishable as an individual thunderstorm system at the surface and aloft by approximately 0946Z (0146 PST, 11 August). Between 0946Z and 1446Z (0146 and 0646 PST) the remaining debris clouds moved eastward and evaporated quickly over extreme east-central Arizona. Consequently, the thunderstorm system remained an identifiable feature in the satellite imagery for approximately 15 hr.

C. Area Affected

During its lifetime, this thunderstorm traveled approximately 500 km and affected an area of nearly $2 \times 10^5$ km$^2$ (see Figure 3). This area includes all of southern Nevada, most of western Arizona, extreme southwestern Utah, and that part of California bordering the Colorado River valley. Contained in this area are numerous Indian reservations, Grand Canyon National Park, the Lake Mead National Recreational Area, some national forests, several wildlife refuges, state parks, the Nevada Test Site (NTS), parts of the U.S. Air Force Gunnery Range in Nevada, the city of Las Vegas, and several smaller communities.

D. Demographics and Thunderstorms

The affected area contains a population of roughly one million people (excluding Phoenix, Arizona, and adjacent suburbs; 1.5 million people). The largest city near the path of the storm was Las Vegas, Nevada, with a standard metropolitan statistical area population of nearly 500,000 people. The storm appears to have reached its maximum intensity over the sparsely populated areas of extreme northwestern Arizona and those parts of Nevada near the Colorado and Virgin Rivers. Available data shows that the greatest damage to property occurred in the area from Moapa to Overton, Nevada (see Figure 3). Local flooding and wind-related damage occurred along much of the storm track.

People seeking new life styles have been moving to the mild, dry climate of the desert southwest. For this and other reasons, the population of the south-western U.S. has been increasing rapidly. For example, the total number of persons in Clark County, Nevada, increased by 70% from 1970 to 1980. During the 50-year period from 1930 to 1980, the population of Clark County increased from 8500 people to nearly 500,000 people. This phenomenal population growth has
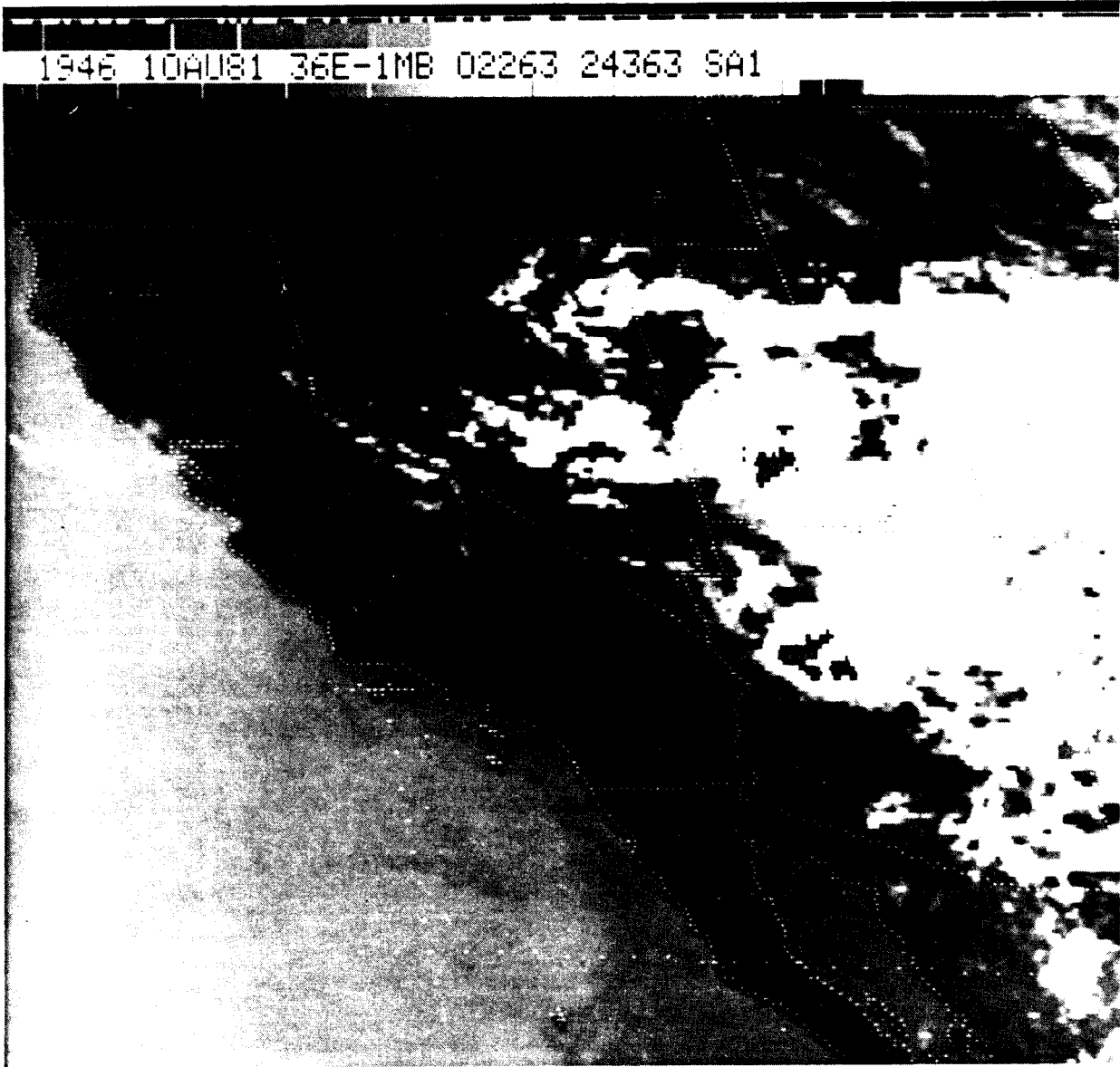
Figure 1. Infrared satellite imagery with MB enhancement for 1946Z (1146 PST), 10 August 1981.

Figure 2. Infrared satellite imagery with MB enhancement for 2046Z (1246 PST), 10 August 1981.

ELY●

CDC: 1450 LST. 2150Z
TB42 W-NW MOVG E LTGCG
SW-N. 1554 LST. 2254Z
TRW-. T SW-S MOVG E.

TPH●

NTS: Wind Towers 1600-1700
LST. 00-01Z wind gusts 35 to
50 mph. Rainfall 0.02" to 0.19".

DRA: 1734 PST: 0134Z TRW-.
PK WND ESE @ 29 mph TE1938
MOVD SE: 0.02" rain.

UTE: 6.0" TO 6.5"
RAIN; HAIL

Moapa-Logandale Area:
1500-1700 LST. 23-01Z.
Much flooding. 500 dairy cows
lost. much property damage.
TRW-A. winds est. 60-80 mph.
2-6" rain.

LVS: 1611-1710 LST: 0011-
0110Z W0X0BN: T-ABN HLSTO
1/4 PK WND NE @ 67 mph 0.15"
rain TRW- through 2155 LST:
0555Z.

TRW+: 1 to 2" rain this corner AZ.

LAS: 1634-2220VLST: 0034-
0620Z W0X0BN: TRW-: PK WND
NE @ 68 mph 0.07" rain massive
power outages.

Lake Mead Area:
Much damage to boats and
harbor facilities.

FLG: 2058 LST. 0359Z
-XM10OVC 1TRW: HLSTO 1/4"
PK WND NNW @ 24 mph.

IGM: 1930 LST. 0230Z BD.
strong sfc winds. wind damage
2130 LST. 0430Z. TRW. local
flooding; AZ HY 68 closed by
flooding W of IGM.

PRC: 2054 LST: 0354Z
E40⊕ 1TRW. PK WND NNW @
67 mph. 0.32" rain.

BLH: 2247 LST: 0647Z
W0X0BDBN PK WND NE @
52 mph.

PHX: 0235 LST: 0953Z CB
OCNL LTGIC W-N MOVG S
WND N 10G19. PK WND 25 mph
0452 LST: 1152Z. RW- RB15.

YUM: 0355 LST. 1055Z 5BDBN
070/14G20 PK WND 30 mph
VSBY N 2mi; CB N-NE DSIPTD.

Figure 3.  Overview of significant surface weather that accompanied the
mesoscale storm system of 10 August 1981.

5

been accompanied by a marked increase in urbanization with its concurrent heightened risk of weather-related catastrophes. Some evidence is available to show that the impact of intense thunderstorms on people and property has been increasing (Randerson, 1976b).

Summer tourists add another dimension. Annually, millions of people visit recreational attractions of the mountainous desert southwest, with summertime being an especially busy period. Many people like to visit, hike, and camp in isolated, sparsely populated areas of Arizona, Nevada, Utah, and southern California. Communication of weather warnings to these individuals is difficult.

The level of experience and awareness of the potential dangers of desert thunderstorms may be minimal with many people who have recently moved to the desert. Upon seeing the dry desert, some may assume that heavy rain, strong surface winds, flash flooding, and lightning don't occur often, or, at least, are not a serious threat. An educational program may be needed to raise awareness.

To compound the developing problem, there has been little documentation of the characteristics, behavior, and the spatial and temporal distributions of desert thunderstorms. Only recent studies, such as those by Sakamoto (1972), Brenner (1974), Hales (1972, 1974, 1975), Idso et al. (1975), and Randerson (1976a, 1977, 1982) have provided information relating to the kinematics and climatology of southwestern desert thunderstorms. Further documentation and research is essential to understand how these storms develop and move so that their occurrence can be forecast more accurately and weather warnings issued in a more timely and effective manner.

## II.  METEOROLOGICAL ANALYSES

A.  Charts

Most of the meteorological charts used have a map background and scale that corresponds with that of the satellite imagery. Consequently, these charts can be overlayed easily onto the satellite imagery so that satellite views of the thunderstorms can be visualized relative to the meteorological analyses.
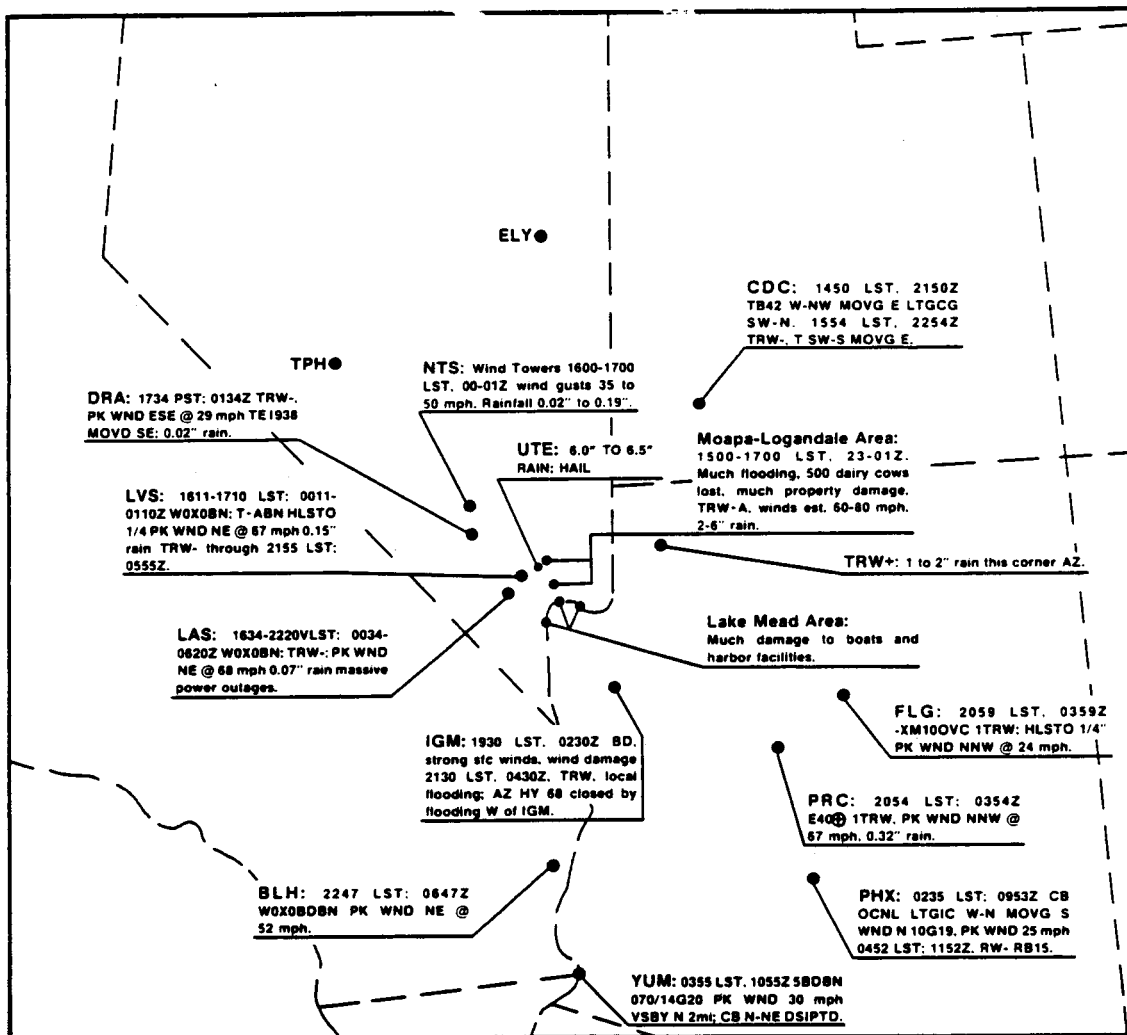
B.  Data

Available meteorological data consists of the standard upper-air observations taken at 0000Z and 1200Z daily as well as hourly and special surface weather observations. Additional data includes hourly radar data, visible and infrared satellite imagery, surface-wind data from a wind tower network on the NTS, detailed cloud-top temperature analyses*, and special analyses of vorticity and divergence**.

---

*   Provided by Mr. J. T. Young, Space Science and Engineering Center, University of Wisconsin, Madison, Wisconsin.
**  Provided by Dr. James E. Arnold, Atmospheric Sciences Division, Marshall Spaceflight Center, NASA, Huntsville, Alabama.

Meteorological data were collected and analyzed for the 4-state area consisting of California, Nevada, Utah, and Arizona. Within this area, the upper-air stations (Figure 4) are approximately 375 km apart. Surface weather data are denser; however, the core of the thunderstorm system did not pass directly over any first-order weather stations. Moreover, the storm developed and traveled within an area lying between upper-air stations. Consequently, surface and upper-air data from the vicinity of the thunderstorm system are scarce; however, some valuable observations were obtained to supplement the satellite imagery and radar data.

Satellite imagery used in this study came from the Geostationary Operational Environmental Satellite (GOES) that was located over the equator at 135°W and at an altitude of nearly 36,000 km. Both visible and infrared (IR) pictures were available for 10 August 1981. The visible sensors scanned the 0.55 to 0.70 $\mu$m light region while the IR images sensed in the 10.5 to 12.6 $\mu$m band. At the satellite subpoint (0.0N, 135W) the best resolution was 1 km for the visible imagery and only 9 km for the IR. One picture was received every 30 min, alternating between visible and IR images, so that the time interval between like pictures was 1 hr until sunset, after which an IR picture was received every 30 min.

The IR imagery available was the MB enhancement which portrays specified ranges of IR black body temperature ($T_{bb}$). Of particular importance were the cloud top areas enclosed by $T_{bb} \leq -32°C$ and by the area enclosed by $T_{bb} \leq -52°C$. To estimate rainfall rates by using satellite imagery, Scofield and Oliver (1977) assumed that precipitation starts to accumulate after $T_{bb}$ reaches -32°C. A cloud shield having $T_{bb} \leq -52°C$ ensures that the system is active and that precipitation is falling over a significant area (Maddox, 1980). Convective clouds with $T_{bb} \leq -58°C$ point to possible overshooting tops. Fujita (1978) has used cloud-top temperatures to study the downburst phenomena.

Air Route Traffic Control Center (ARTCC) radars detect thunderstorm activity. In the western U.S., the National Weather Service compiles a summary of this weather-related radar-echo activity once each hour on approximately the half hour. The summarized data are transmitted over a RAFAX network 15 min later. It is important to emphasize that ARTCC radars were designed and sited to provide the best possible detection of aircraft. Furthermore, these radars are equipped with special circuitry, such as, sensitivity time control and circular polarization, to specifically remove most weather related targets. Such design qualities do not provide for optimum detection of precipitation. Despite these limitations, the ARTCC radars are capable of providing much useful weather data (Benner, 1965). However, Ronne (1971) concluded that some ARTCC radars probably display only moderate or greater precipitation intensities.

High mountainous terrain can restrict the detection of moist convection by radar. However, the thunderstorm system of interest developed and moved through an area where the probability of radar detection of surface precipitation during summertime is 80 to 90 percent (e.g., see Randerson, 1976b). This probability decreases to 70 percent in northwestern Arizona.

## C. Pre-storm Conditions

### 500-mb Flow

On the morning of 10 August 1981, atmospheric conditions over Utah, Arizona, and eastern Nevada were favorable for thunderstorm development. The potential for intense thunderstorms was present. Figures 4 and 5 illustrate the important evolving meteorological situation. Figure 4, the 500-mb chart, is represe.ta-tive of the pre-storm meteorological conditions in the mid and upper troposphere at 1200Z (0400 PST) on 10 August 1981. The most important feature in this figure is the sharp, southward-moving trough oriented east-west along the Nevada-Idaho border. Accompanying the trough is a strong cyclonic vorticity field (dashed lines). Notice, in particular, that the vorticity contours are tightly packed between DRA and ELY with the axis of maximum relative vorticity advection oriented along a line from SLC to north of the NTS. Areas of positive vorticity advection are normally associated with upward vertical motion (Petterssen, 1956). Flow in the upper troposphere contained a small jet stream that was essentially parallel to the 5880-m contour in Figure 4. Maximum wind speeds accompanying this west-northwesterly jet were roughly 30 m/s (50 kts). Intense thunderstorm development took place to the south of the jet stream axis in early afternoon.

### Low-Level and 850-mb Flow

Meteorological conditions in the lower troposphere are illustrated by Figure 5, the 850-mb chart for 1200Z. The height contour analysis shows a low center between ELY and DRA. The contour field indicates that flow with a strong southerly component should have existed over southwestern Utah, northwestern Arizona, and southern Nevada. Surface winds at 1200Z (0400 PST) in the Las Vegas area were southerly 7 to 11 m/s (15 to 25 mph). Cedar City and Milford, Utah, and Prescott and Grand Canyon, Arizona, all had surface winds driven by local thunderstorm and rainshower activity. In general the 850-mb flow regime appears to have been imperfectly balanced in the geostrophic sense. Both the 1200Z and 1800Z (0400 and 1000 PST) winds aloft observations from DRA (elevation 1,100 m) detected light (3 to 5 m/s) southerly flow from the ground to 1,300 m (4,000 ft) above the ground.

By late afternoon the low-level flow regime over Nevada, Utah, and north-western Arizona could be separated into three distinctly different air masses. Northern Nevada was covered by a polar air mass located north of a frontal zone that extended westward across central Utah into central Nevada (Figure 5). In Nevada this frontal zone was moving slowly southward. A hot, dry continental tropical air mass was spreading eastward from southern California across southern Nevada as maritime tropical air over extreme southeastern Nevada receded slowly eastward. The boundary between these two tropical air masses could be identified by a marked dew-point temperature gradient at the surface. This "dew-point front" extended north-south over southern Nevada.

### Low-Level Moisture

Low-level moisture available to fuel thunderstorms is portrayed in Figure 5 by the dashed lines representing dew-point depression at the 850-mb level. The most significant feature in this diagram is the very tight moisture gradient over southern Nevada. Very dry air was present over most of California while

Figure 4. The 500-mb chart for 1200Z (0400 PST), 10 August 1981. Height contours in 10's of meters are solid lines and the relative vorticity field (X $10^{-6}$ $s^{-1}$) is portrayed by the dashed lines. Data are plotted in the standard format. The map background is the same as that in all the satellite images.

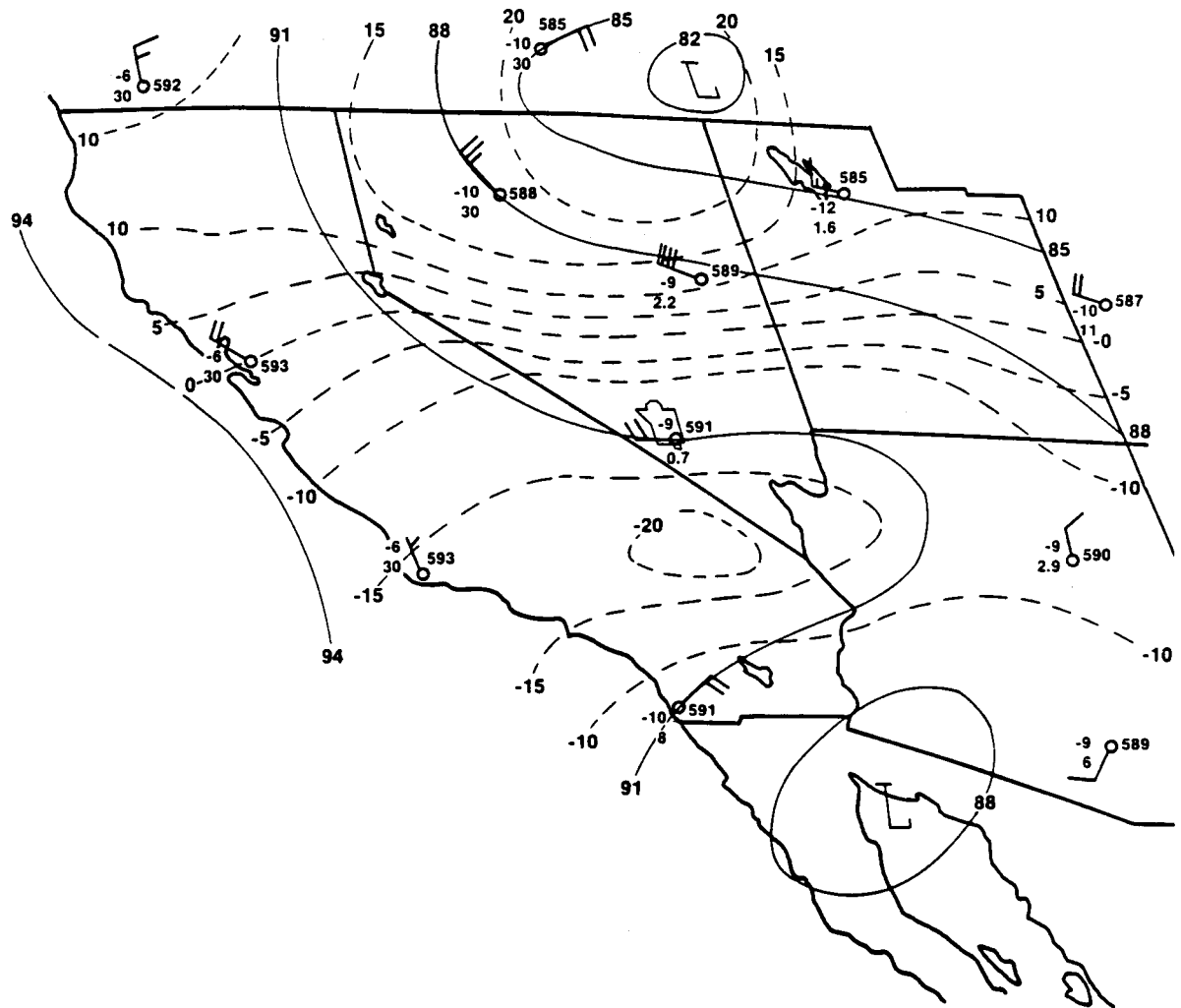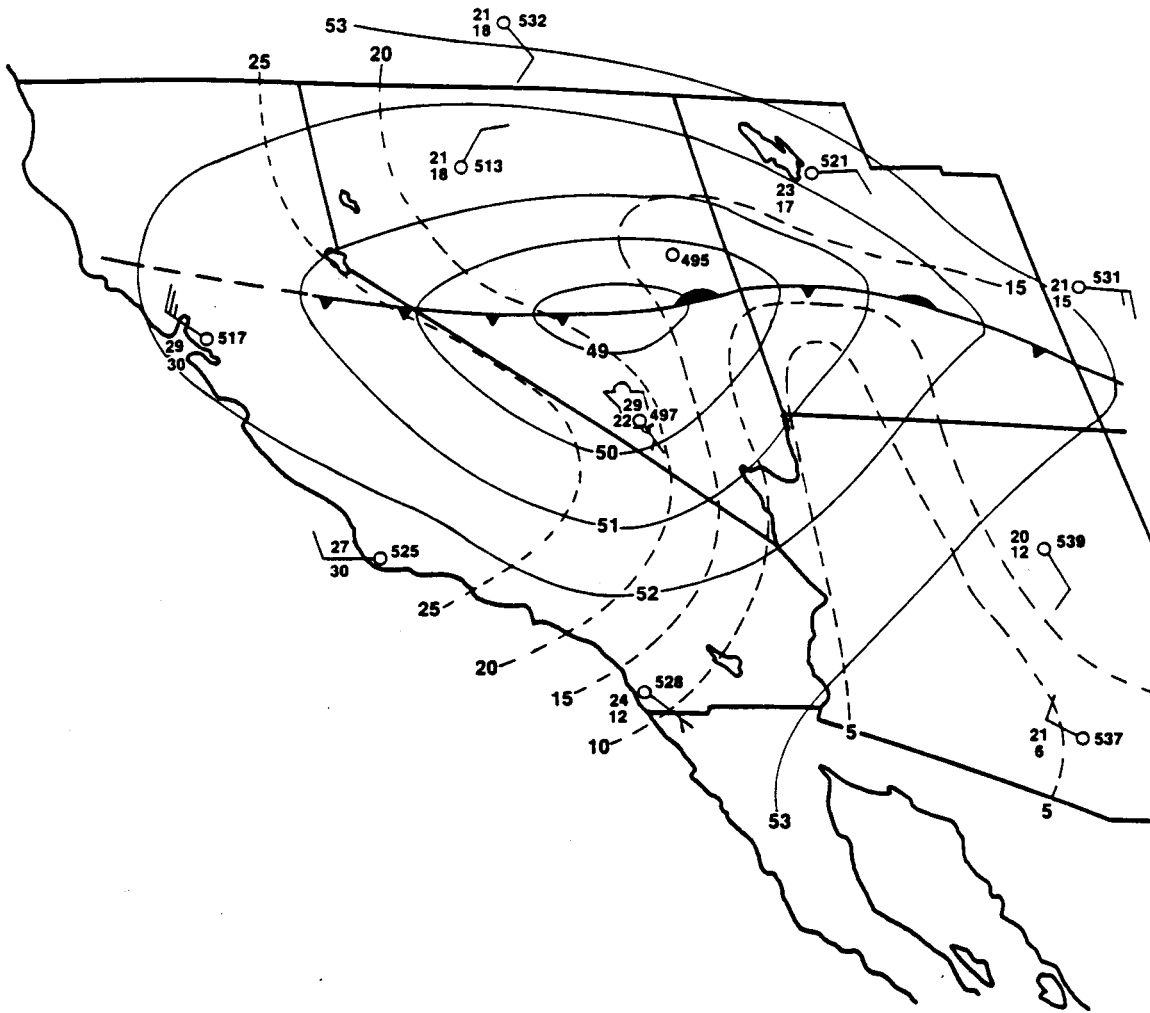Figure 5. The 850-mb chart for 1200Z (0400 PST), 10 August 1981. Height contours in meters are solid lines and the dashed lines represent dew-point depression (°C). Data are plotted in the standard format. The map background is the same as that for all the satellite images.

10

the axis of maximum moisture content ($T-T_d \leq 5°C$) extended from western Arizona northward into southwestern Utah. This positioning is based on the plotted data, on satellite and radar data, and on observed low clouds and precipitation occurring within the 5°C departure contour. Based on the plotted temperature data and on the position of the isodrosotherms over northwestern Arizona, mixing ratios of 10 to 15 g/kg may have been available to the generating thunderstorm system at the 850-mb level. Surface mixing ratios at Cedar City and in Las Vegas were 10 to 12 g/kg prior to storm development.

## Divergence

A computer-generated analysis of the 1200Z, 850-mb divergence field showed a pronounced area of convergence (nearly $-2 \times 10^{-4}s^{-1}$) centered just north of the NTS and covering all the southern half of Nevada and southwestern Utah. A similar analysis for the upper troposphere (200-mb level) showed an east-west oriented axis of strong divergence ($10^{-4}s^{-1}$) centered over southern Utah and southeastern Nevada. These divergence fields along with the positive vorticity advection at the 500-mb level (Figure 4) implies a well-developed area of upward motion throughout most of the troposphere over southern Nevada and southwestern Utah. In fact, computations of vertical motion based on the continuity equation and on the calculated divergence field at the surface, 850-, 700-, 500-, and 200-mb levels for 1200Z showed a deep layer (surface to 12,000 m) of upward motion of 10 to 15 cm/s located south of Ely, Nevada. Coupled with this upward motion and the southward movement of the upper-air trough, surface heating during the day, and the advection of low-level moisture into southwestern Utah, the stage was set for the development of intense thunderstorms.

## Atmospheric Stability

The 1200Z vertical temperature sounding for DRA on the morning of 10 August (Figure 6) shows that the atmosphere was conditionally unstable from near the 1500-m (5,000-ft) level to near the 11,000-m (35,000-ft) level. A small stable layer was detected near 6,100 m (20,000 ft). The tropopause was near the 15,000-m (48,000-ft) level where the temperature was roughly -64°C. A region of relatively stable air existed between the 11,000-m (35,000-ft) level and the tropopause. In the 12-hour period between 1200Z and 0000Z (11 August) the DRA temperature sounding changed little (Figure 7). Below the 6,100-m level there was essentially no change except for strong heating near the surface. Above 6,100 m there was a general warming of 2°C up to near the 12,000-m (40,000-ft) level. The stable layer near 6,100 m vanished and a relatively stable layer existed between the 12,000-m level and the tropopause.

At 1200Z, 10 August 1981, the stability indices calculated from the DRA sounding (Figure 6) showed that the atmosphere was unstable. The K-factor (George, 1960) was 26 and the lifted index (Stackpole, 1967) was -3. But the low-level air over southern Nevada was relatively dry (Figure 5). Instability might have been increased by the advection of the low-level moist (and cooler) air over northwestern Arizona into southeastern Nevada during the morning hours. Strong surface heating of this shallow moist layer could have created a large negative lifted index. Available data indicate that mean, low-level mixing ratios as high as 14g/kg could have existed over northwestern Arizona. In addition, surface heating could have raised the mean low-level potential temperature to 45°C or more. Based upon these two assumptions, the lifting condensation level would have been near the 700-mb level; a value supported by
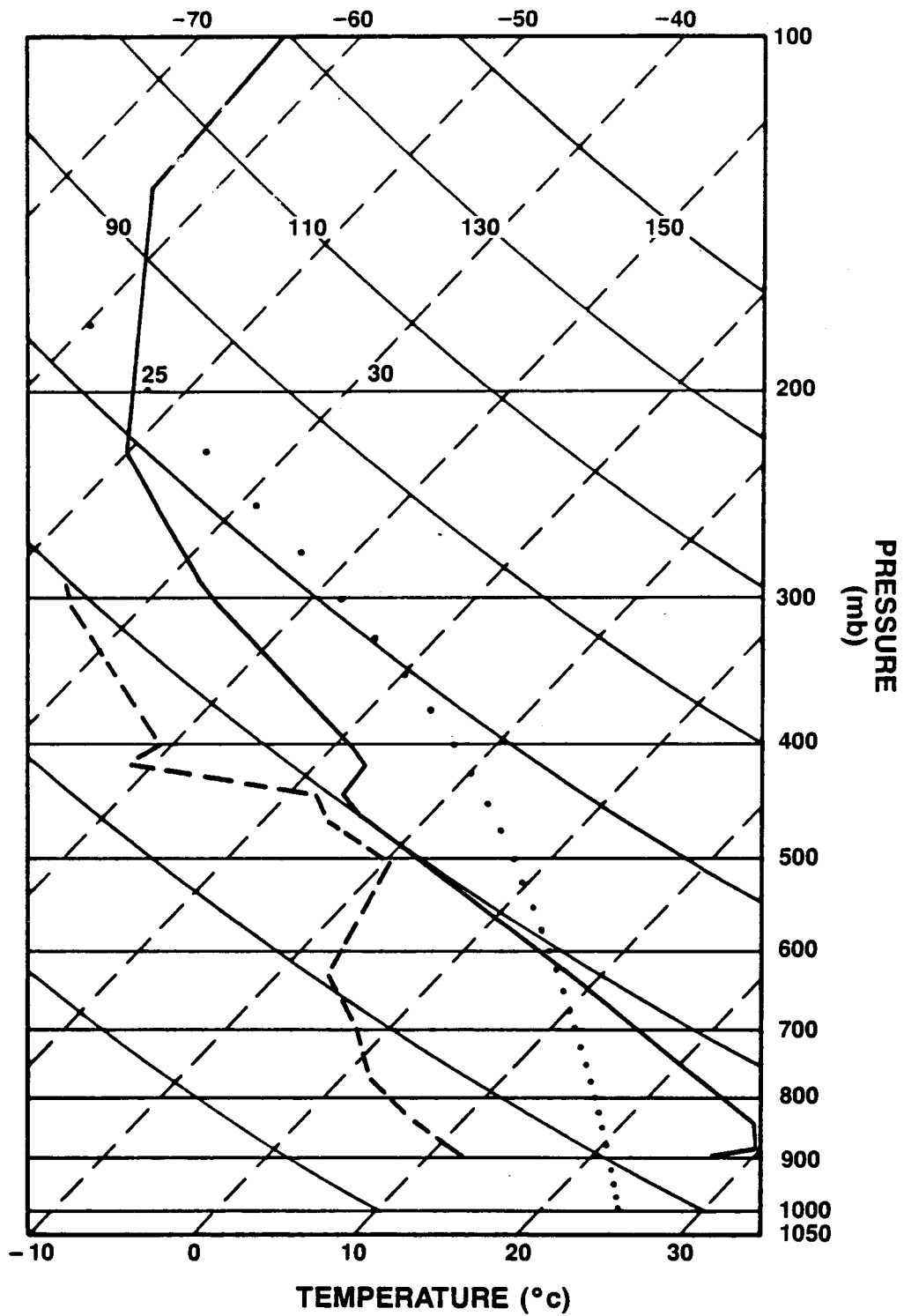
11

Figure 6. Skew T-log P diagram for Desert Rock, Nevada, (DRA) for 1200Z (0400 PST), 10 August 1981.
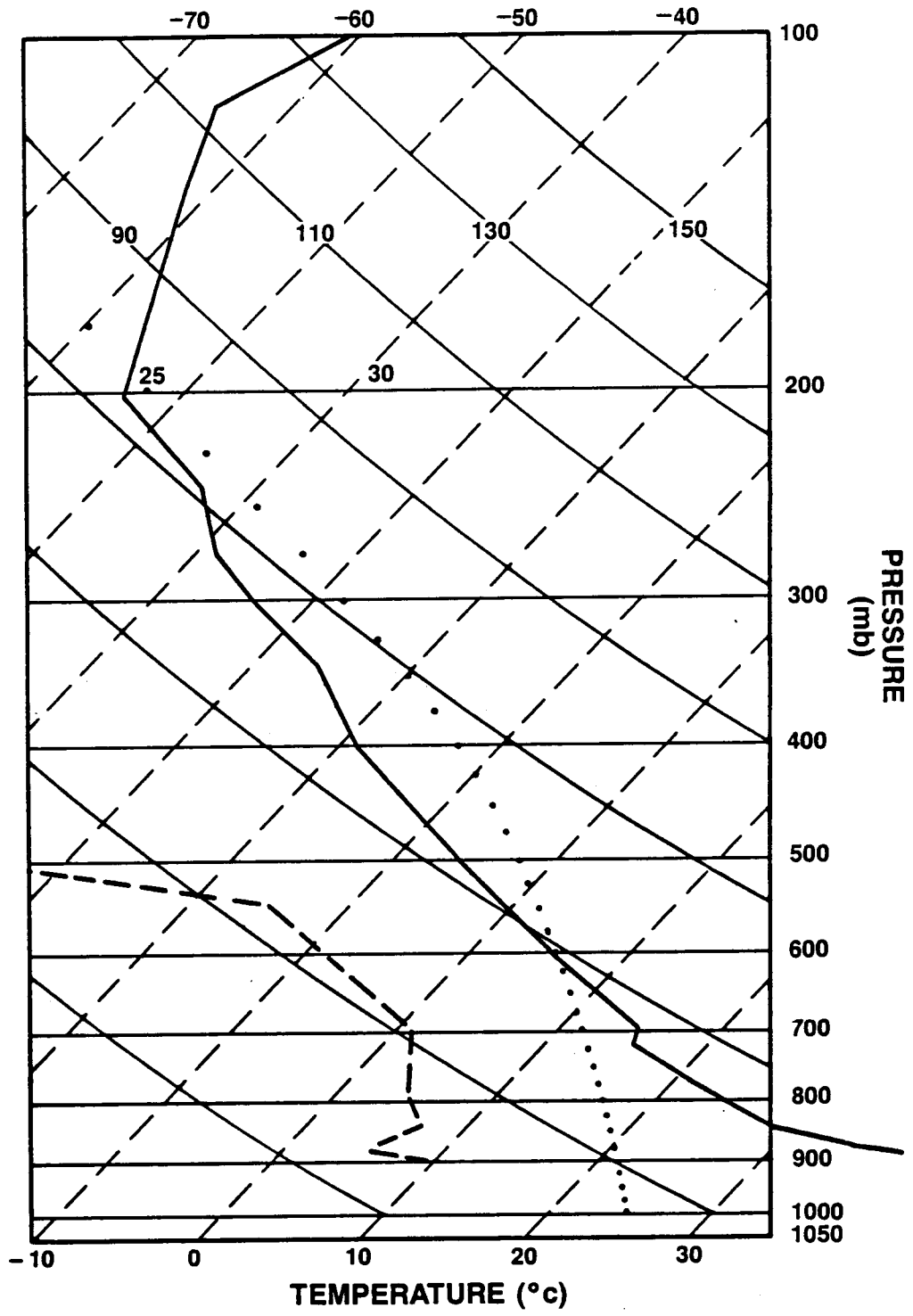
12

Figure 7. Skew T-log P diagram for Desert Rock, Nevada, (DRA) for 0000Z, 11 August 1981, or 1600 PST, 10 August 1981.

surface observations of the bases of the thunderstorms that developed in the Las Vegas area (see paragraph F). Based on the 0000Z (11 August) sounding, the lifted index over southern Nevada and northwestern Arizona could have been -8 with $\theta_e$ =26°C. These conditions would have produced a very large area of positive buoyancy throughout the middle and upper troposphere. The tops of the thunderstorms would have been near the 13,500-m (45,000-ft) level with cloud-top temperatures of -60° to -65°C. These values are consistent with satellite observations (see paragraph K).

D. Storm Development

After 2000Z (1200 PST), thunderstorms started to develop rapidly and grow in areal extent south of Ely. This development is portrayed neatly by changes in the clouds shown in the infrared satellite pictures of Figures 1 and 2. In Figure 1, the two large cumulonimbus clouds in eastern Nevada had cloud-top temperatures of -42° to -52°C, corresponding to an altitude range of roughly 10,500 to 11,700 m (34,000 to 38,000 ft) above mean sea level (MSL). One hour later (Figure 2), the two individual cumulonimbus had consolidated into one large cloud mass and the cloud-top temperature had cooled. The dark-gray shading corresponds to equivalent black body temperatures of -53° to -58°C or approximately 11,700 to 13,000 m (38,000 to 42,000 ft) MSL. Two very cold tops are seen as black spots within the dark gray shading. These two points have a $T_{bb}$ of -63° to -80°C. Based on a computer analysis of cloud-top temperatures and on the 0000Z (1600 PST) temperature sounding for DRA (Figure 7), the $T_{bb}$ was near -65°C.

The horizontal area of the cloud tops in Figure 1 (light-gray shading $T_{bb} \le$ -32°C) is nearly $10^4$ $km^2$.* One hour later this area grew to $2 \times 10^4$ $km^2$ and the new colder cloud tops ($T_{bb} \le$ -52°C) covered an area of roughly $4 \times 10^3$ $km^2$*. The $T_{bb} \le$ -32°C is near the 300-mb level (see Figure 7). Mass divergence of the cloud top with this temperature can be calculated from $(A)^{-1}$ $(dA/dt)$, yielding $1.85 \times 10^{-4} s^{-1}$ near the 300-mb level. This value represents an approximate mass balance with the convergence derived for the 850-mb level (see Divergence section).

Radar data collected at approximately 2030Z (see Appendix A) corresponds closely with the 2046Z (1246 PST) satellite picture (Figure 2). Radar reflectivities indicated a "very heavy" thunderstorm (TRW++) below the cold ($T_{bb}$=-53° to -58°C) cloud tops. A TRW++ corresponds approximately to VIP level 4 or to 2.2 to 4.5 in/hr (56 to 144 mm/hr) of precipitation at the ground (Grebe, 1982). No such precipitation amounts were reported or measured below this thunderstorm; however, one station under this echo, Key Pittman, Nevada (KEY), did receive a daily total of 1.5 in (38 mm). A post-storm weather summary prepared by J. W. Corey, a Lead Forecaster at the Reno, Nevada, WSFO, indicated that 0.7 in (17.8 mm) of rain fell at Key Pittman in 20 min for a rainfall rate of 2.1 in/hr (53 mm/hr). Radar reports indicated that the maximum cloud top of this TRW++ was 14,000 m (46,000 ft) MSL. This altitude is consistent with that estimated from 0000Z (1600 PST) DRA sounding (Figure 7) and with the coldest (-65°C) cloud top estimated from the satellite imagery.

---

* Not corrected for parallax.

14

Cumulonimbus development in eastern Nevada coincided with several important developments in the atmosphere. It appears to have occurred in a region of positive vorticity advection, strong upward motion, and low-level moisture convergence. It took place ahead of a surface wave on a cold front, and it may have been enhanced by intense surface heating. For example, the maximum temperature in LAS before the thunderstorm was 42°C (107°F).

E. Mature Stage

Between 2000Z (1200 PST) and 0200Z (1800 PST), the convective, mesoscale weather system continued to grow in horizontal area and cloud-top temperatures continued to cool. Based on these two measures, the storm appears to have reached maximum intensity between approximately 0000Z (1600 PST) and 0400Z (2000 PST). Figures 8 and 9 show the IR imagery for the storm at 2346Z and 0146Z (1546 and 1746 PST) respectively.

Maddox (1980) used size and duration criteria to identify a Mesoscale Convective Complex or MCC (Table 1a). His requirement that a large part of MCC cloud shields have a $T_{bb} \leq -52°C$ indicates that the system is active and that precipitation is falling over a large area. According to Maddox, the scale of an MCC is huge relative to individual thunderstorms. For example, mature air mass thunderstorms have a cold ($T_{bb} \leq -32°C$) cloud-shield area of roughly 700 $km^2$. Multicell thunderstorms have corresponding average cloud-top areas of 1400 $km^2$ (Reynolds and Vonder Haar, 1979). In Table 1a, notice that the size of an MCC cloud shield exceeds that of an individual thunderstorm by more than two orders of magnitude.

Based on the criteria listed in Table 1a, the convective weather system of 10 August appears to qualify marginally as a small MCC. Figure 10 shows that size criteria A and its duration requirement are met. The area enclosed within the -32°C isotherm is $10^5$ $km^2$ or greater for at least 8 hr. Size criteria B is met for only 5 hr, one hour short of the minimum 6-hr duration criteria. The contiguous cloud shield with $T_{bb} \leq -32°C$ reached a maximum size of approximately 2.1 X $10^5$ $km^2$ at 0300Z (1900 PST). At this time the shape criteria (Table 1a) was met. Consequently, the only physical requirement not met was the duration criteria for size category B which terminated one hour early.

Bartels et al. (1984) proposed a different set of criteria for mesoscale convective systems (Table 1b). The storm of 10 August appears to have satisfied most of these criteria. The duration scale was satisfied, however, the length scale of the ≤ 52°C contiguous area was exceeded slightly.

Mesoscale space and time scales were defined by Orlanski (1975). He defined β scale phenomena as having characteristic times of 5 to 24 hr and horizontal scales of 20 to 200 km. The storm of 10 August had a duration of approximately 15 hrs. The maximum horizontal extent of the IR $T_{bb} \leq 52°C$ area was nearly 250 km from 0146 to 0246Z (1746 to 1846 PST). Maddox (1980), Bartels et al. (1984), and others have recognized that the ≤ 52°C cumulonimbus cloud-top isotherm is often associated with deep, precipitating convective clouds. Consequently, it is selected here to represent the spatial scale of the storm system. For most of the storm lifetime the cross-sectional length of the area enclosed within this isotherm was <200 km.
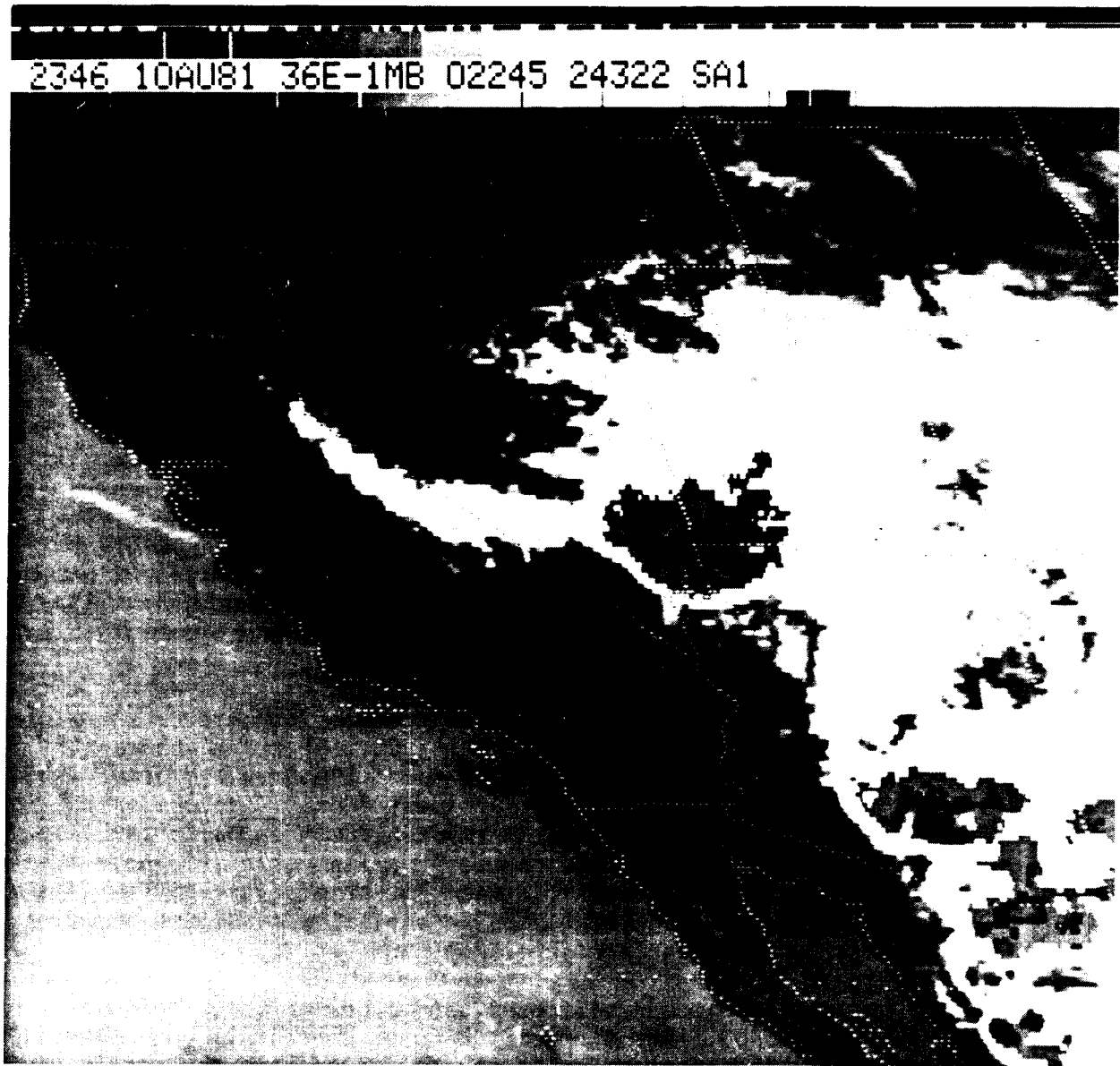
15

Figure 8. Infrared satellite imagery with MB enhancement for 2346Z (1546 PST), 10 August 1981.
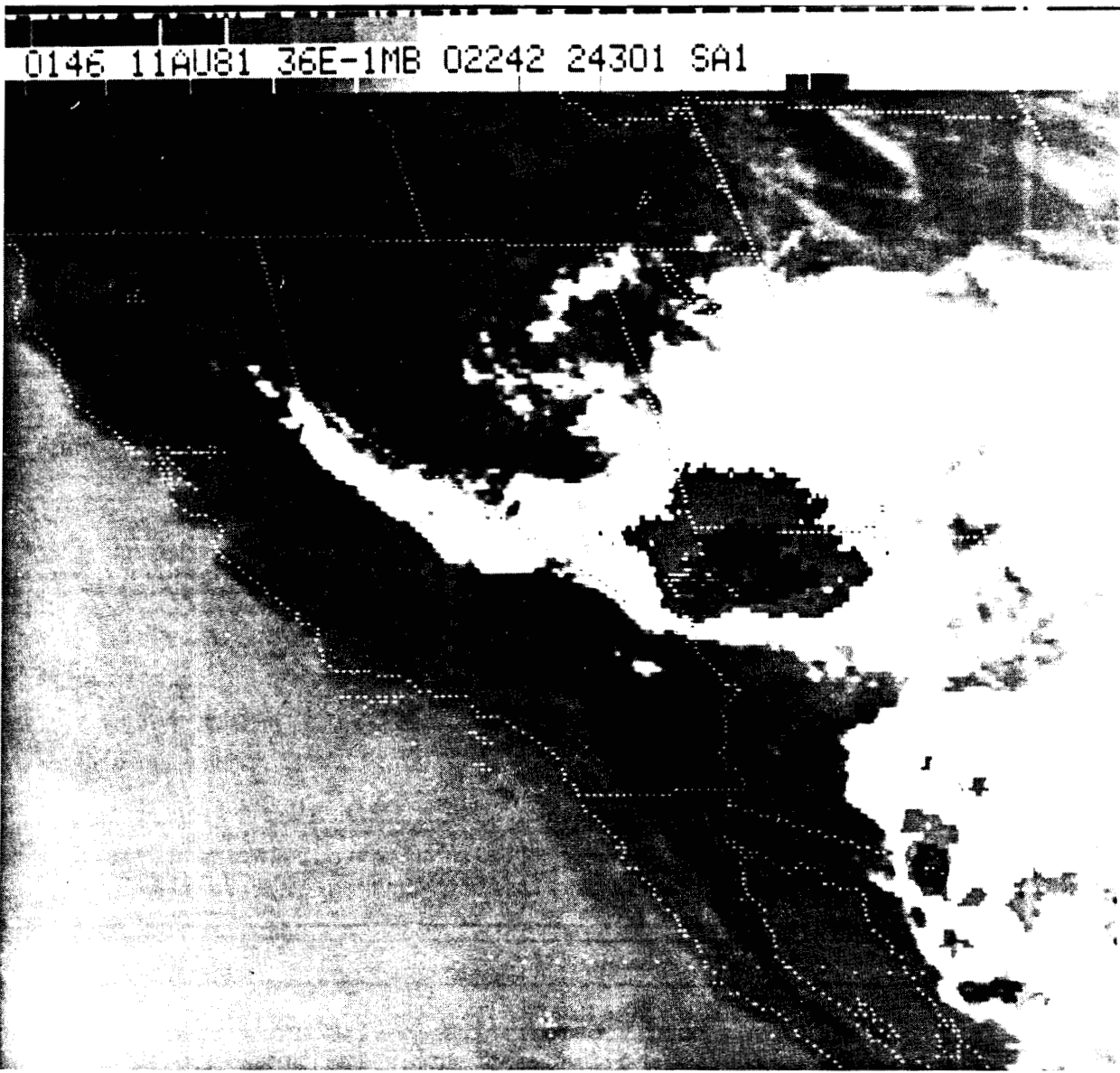
Figure 9. Infrared satellite imagery with MB enhancement for 0146Z, 11 August 1981, or 1746 PST, 10 August 1981.

Table 1a.    Criteria for a Mesoscale Convective Complex (Maddox, 1980).

<u>Physical Characteristics</u>

Size:        A -  Cloud shield with continuously low IR temperature $\leq -32°C$ must have an area $\geq 1,000,000$ km².

             B -  Interior cold cloud region with temperature $\leq -52°C$ must have an area $\geq 50,000$ km².

Initiate:    Size definitions A and B are first satisfied.

Duration:    Size definitions A and B must be met for a period $\geq 6$ hr.

Maximum      Contiguous cold cloud shield (IR temperature $\leq -32°C$) reaches
extent:      maximum size.

Shape:       Eccentricity (minor axis/major axis) $\geq 0.7$ at time of maximum extent.

Terminate:   Size definitions A and B no longer satisfied.


Table 1b.    Mesoscale Convective System Criteria based upon the analysis of
             enhanced IR satellite imagery (after Bartels <u>et al</u>., 1984).

| <u>Characteristic</u> | <u>Criterion</u> |
|---|---|
| Length: | Length scale of the <-52°C contiguous enhanced area on satellite image is <250 km. |
| Duration: | Minimum length scale is maintained for at least 3 hr. |
| Initiation: | The length scale criterion is first met. |
| Maximum Extent: | Contiguous cold cloud shield (IR temperature <-52°C) reaches maximum size. |
| Termination: | The length scale criterion is no longer met. |

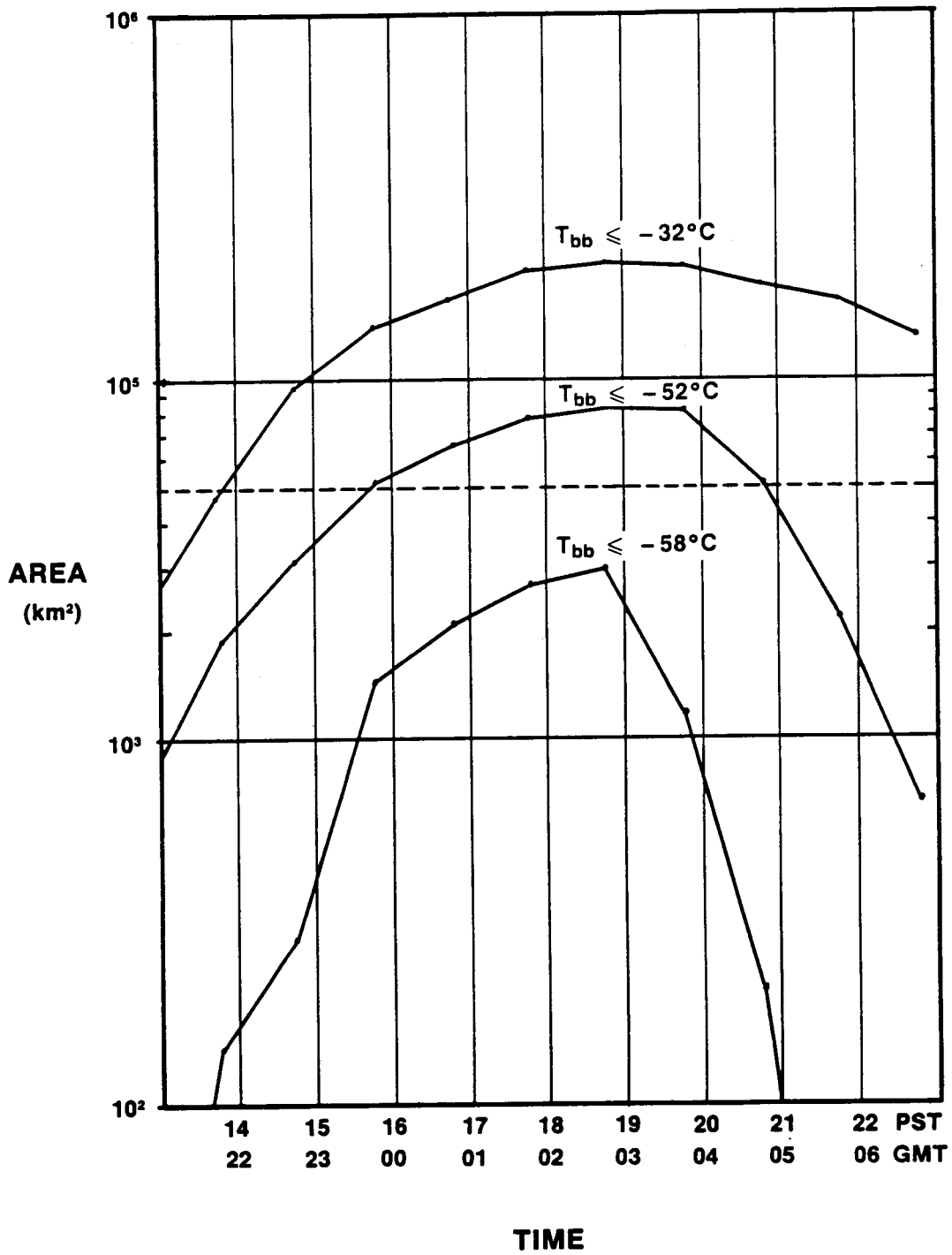Figure 10. Graphical representation of the temporal change in the total area enclosed within three separate equivalent black body temperature ($T_{bb}$) regimes visible in the infrared satellite images with MB enhancement.

Based on the above definitions and observations, it is concluded that the storm of 10 August was an MCC. Indeed, it may have been a mini-MCC, but the duration, size, and weather accompanying this large convective cloud cluster were significant from a meteorological, hydrological, and societal perspective.

F. Upper-Air Analyses

Upper-air sounding data for 0000Z (1600 PST) help portray the atmospheric-flow regime associated with the developing MCC. The 0000Z (1600 PST), 850-mb chart (Figure 11) shows that the well-developed frontal wave present at 1200Z (0400 PST, Figure 5) had maintained its intensity and moved slowly eastward during the intervening 12-hr period. The cold front moved southward across Nevada, bringing strong northeasterly flow to the eastern slopes of the Sierras. These winds induced orographic cumulonimbus over the Sierras (see Figures 8 and 9).

In the upper troposphere (Figure 12), at 0000Z (1600 PST), a deep closed low was located just northwest of SLC at the 200-mb level. Figure 12 represents the flow near the top of the MCC. The contour analysis in this figure indicates that the flow over Utah and Nevada was strong westerly with a region of difluence located over the MCC generation area. Based on the contour analysis, geostrophic wind speeds in the area between ELY and DRA are likely to have been near 25 m/s (50 kts). Consequently, the MCC developed to the right of a small jet and below an area of upper-tropospheric difluence.

A weak, low-level, southwesterly jet probably existed over southern Nevada at 0000Z (1600 PST). The 0000Z winds-aloft sounding from DRA showed that below 12,000 ft (4,000 m) MSL the maximum wind speed was 12 m/s (23 kts) at both the 1,800- and 2,100-m (6,000- and 7,000-ft) levels MSL or approximately 900 to 1,200 m (3,000 to 4,000 ft) above ground level (AGL). Wind towers on high (2,100-m MSL) terrain in the northern part of the NTS confirmed the existence of such wind speeds. Wind directions were generally southwesterly. Prior to the arrival of the strong surface outflow from the thunderstorm, surface winds at two weather stations in the Las Vegas valley were reported to be southwesterly 5 to 13 m/s (10 to 25 kts). Boundary-layer theory predicts that above the ground, wind directions should have been southwesterly at slightly faster speeds (e.g. Randerson, 1984).

Vertical wind shear may have been a contributing factor in the development and maintenance of the MCC. The only winds-aloft data near the MCC are those from the 0000Z (1600 PST) DRA rawinsonde (Table 2). Just prior to 0000Z, the westward edge (Figure 8) of the MCC was 55 km east of DRA while the center of the storm was at a distance of roughly 220 km. Based on ceiling observations during the thunderstorm activity at DRA, LAS, and LSV, it can be assumed that the base of the MCC was near 10,000-ft (3050-m) MSL. Using this assumption, the data in Table 2 indicate that the mean subcloud winds were approximately 215° at 10 m/s while the mean environmental cloud-layer winds were 300° at 12 m/s. The difference between these two mean winds yields 85° of veering between the sub-cloud winds and the environmental cloud-layer winds. Storm movement was from 345° at 15 m/s, or 45° to the right of the direction of the mean environmental cloud-layer winds and at a speed approximating wind speeds in the middle troposphere. Consequently, the subcloud air layer had a strong component of relative motion toward the approaching storm. Such motion probably caused

20

Figure 11. The 850-mb chart for 0000Z, 11 August 1981 (1600 PST, 10 August).
Height contours in 10's of meters are solid lines. Data are plotted
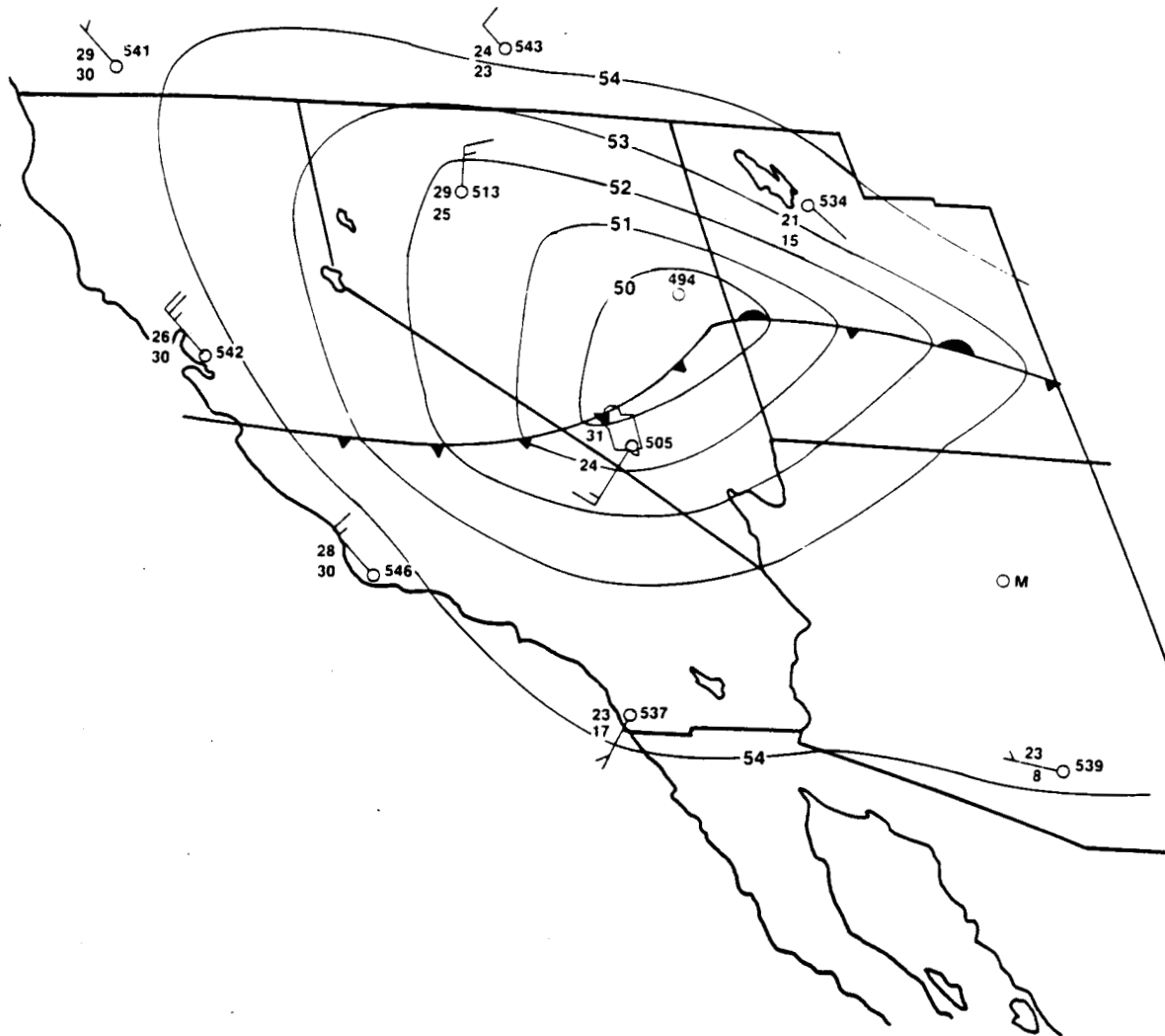in the standard format. The map background is the same as that for
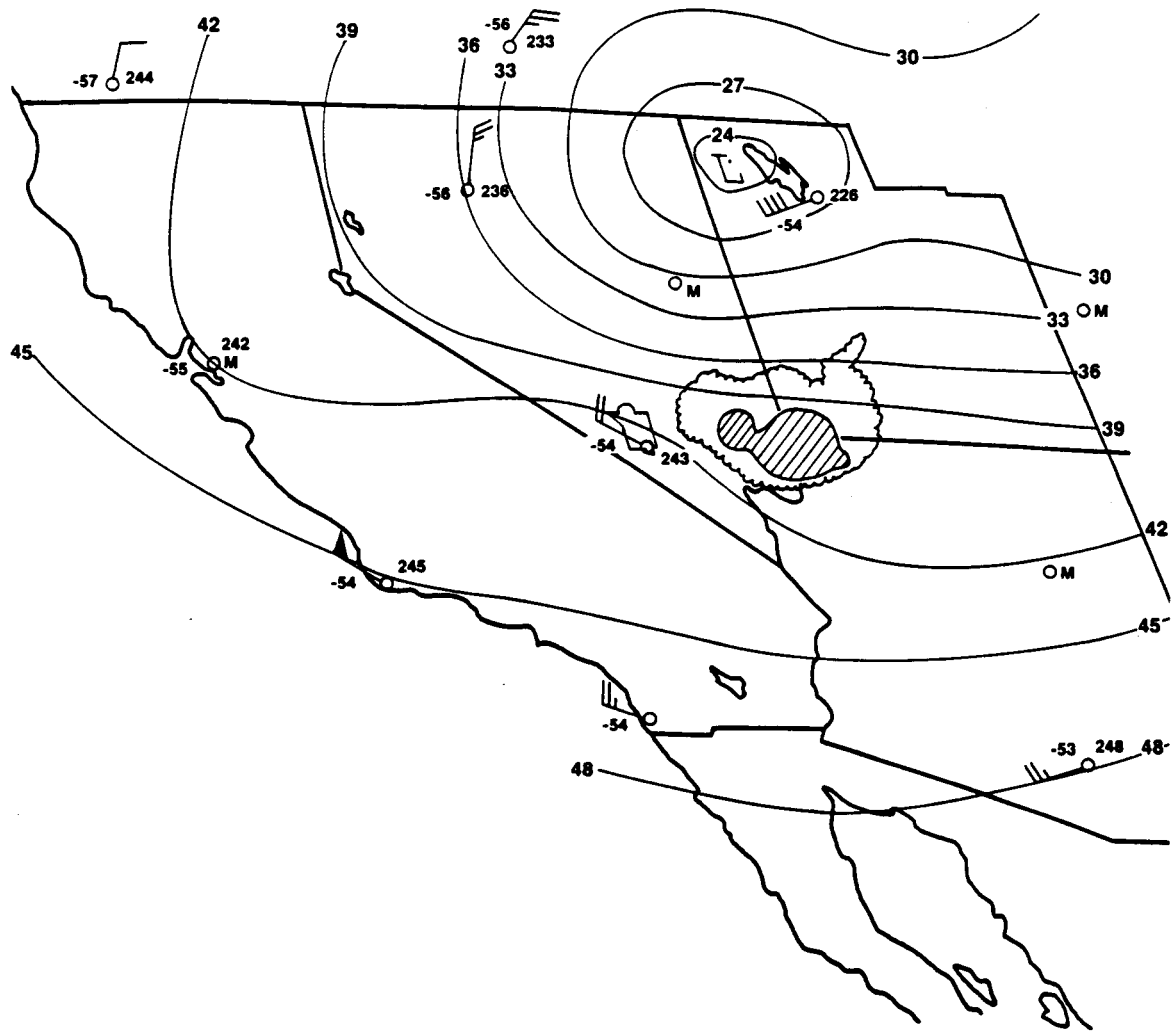all the satellite images.

Figure 12. The 200-mb chart for 0000Z, 11 August 1981 (1600 PST, 10 August). Height contours in meters are the solid lines. The position of the MCC is portrayed by the scalloped area. The scalloped contour represents $T_{bb}$ =-53.2° to -58.2°C, and the shaded area $T_{bb}$ =-59.2° to -62.2°C.

Table 2.    The 0000Z winds aloft from Desert Rock, NV (DRA), elevation 3,298 ft MSL. The MCC cloud base is assumed to be at an altitude of 10,000 ft (3050 m) MSL. All elevations (H) are above mean sea level. The tropopause was located just below the 50,000-ft (15,240-m) level.

| Sub-cloud Winds | | | Environmental Cloud-layer Winds | | |
|---|---|---|---|---|---|
| H | | DDD/SS | H | | DDD/SS |
| ft(x10³) | km | deg/ms⁻¹ | ft(x10³) | km | deg/ms⁻¹ |
| Sfc | 1.0 | 180/9 | 15 | 4.6 | 290/11 |
| 4 | 1.2 | 215/9 | 20 | 6.1 | 310/14 |
| 5 | 1.5 | 215/10 | 25 | 7.6 | 305/16 |
| 6 | 1.8 | 215/12 | 30 | 9.1 | 300/15 |
| 7 | 2.1 | 215/12 | 35 | 10.7 | 310/13 |
| 8 | 2.4 | 215/11 | 40 | 12.2 | 305/11 |
| 9 | 2.7 | 210/10 | 45 | 13.7 | 285/7 |
| 10 | 3.0 | 240/9 | 50 | 15.2 | 015/4 |

pronounced enhancement of the flow of warm, moist air into the storm, thereby helping vigorous updraft motion that might have been initiated by strong thermal instability. The large vertical wind shears observed in the environmental cloud-layer winds near intense mid-western states thunderstorms (e.g., see Maddox, 1976) were not observed in this case.

G.  Surface Wind

    As is typical with intense thunderstorms, a well-defined wind shift or gust front accompanied the MCC. A gust front is the leading edge of a thunderstorm downdraft that spreads out horizontally near the ground. The gust front is the interface between the warm, moist air flowing toward the storm and the cold, moist downdraft air flowing out of the storm. The downdraft appears to have its origin in the mid-troposphere where dry environmental air can be drawn into the storm. As this air enters the rear of the storm it receives precipitation from above and is cooled further by evaporation. This cooling increases the negative buoyancy of the dry air, causing the chilled air to accelerate toward the ground.

    Strong outflow winds were detected along the storm track (Figures 3, 13 and 14). At 2355Z (1555 PST) the weather station closest to the MCC (Nellis AFB, LSV) experienced a wind shift from the south-southwest at 7 m/s (14 kts) to the north-northeast at 21 m/s (40 kts) with gusts to 26 m/s (51 kts) at 0007Z (1607 PST). A peak wind gust of 30 m/s (58 kts) occurred at 0017Z (1617 PST). Twenty-seven minutes after the gust front struck LSV it reached McCarran International Airport (LAS) at 0034Z (1634 PST). A peak wind gust of 30 m/s (59 kts) was measured at LAS at 0040Z (1640 PST). The outflow arrived at
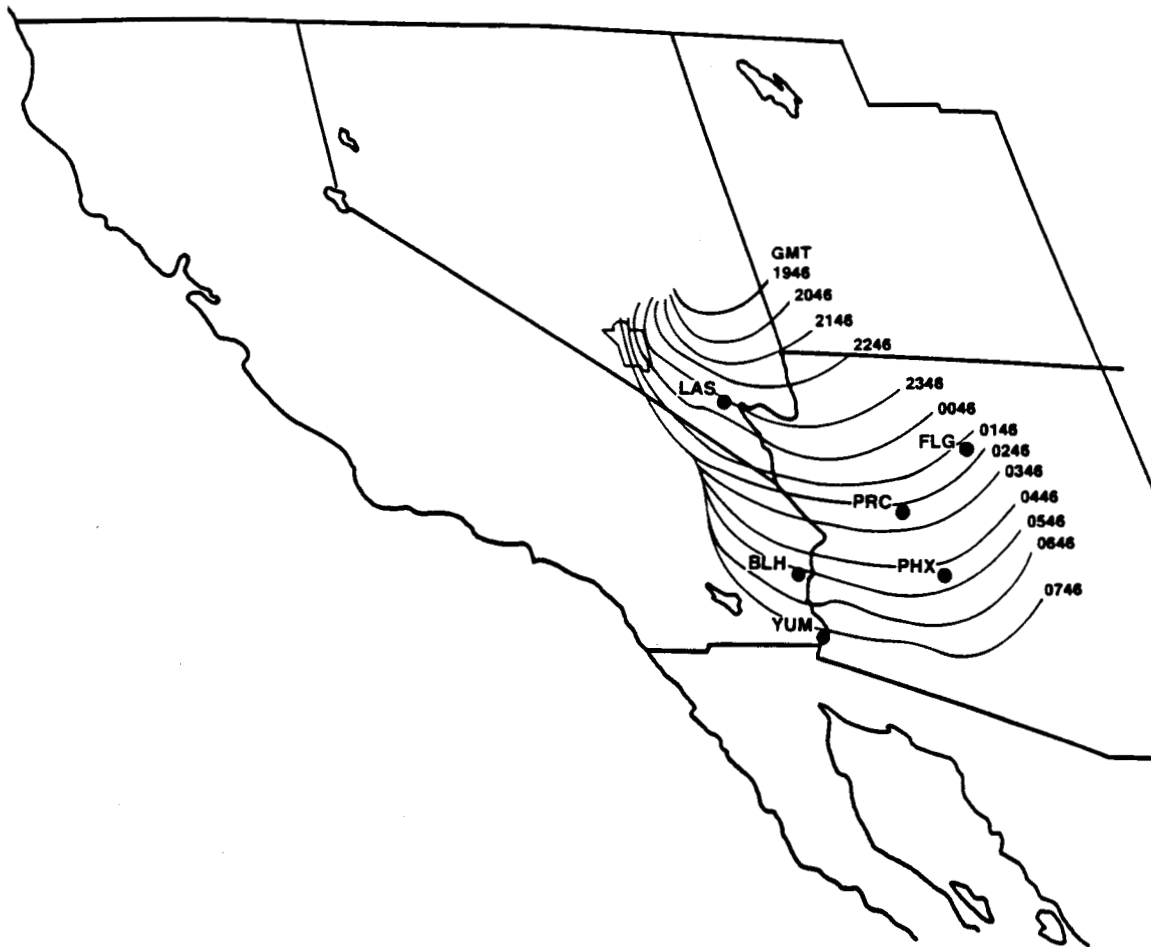
Figure 13. Estimated hourly positions of the leading edge of the strong outflow winds from the MCC of 10 August 1981. Times are in GMT; subtract 8 hrs to get PST.
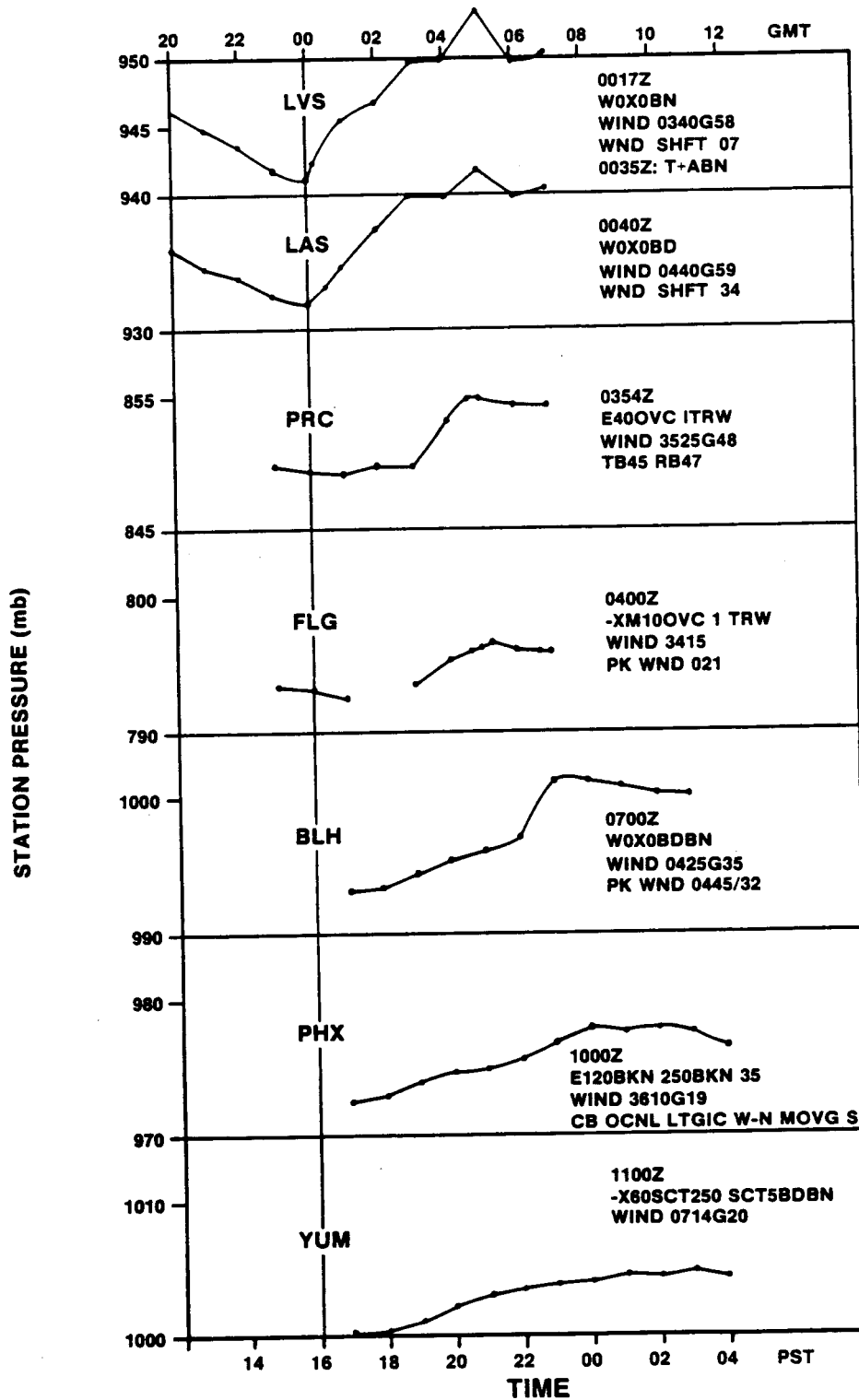
Figure 14. Plots of hourly and special reports of station pressure and extreme weather conditions at selected stations along the path of the MCC of 10 August 1981.

Prescott, Arizona, approximately 3 hr later with a peak wind gust from the north of 25 m/s (48 kts). As the storm moved southward the gust front arrived at Blythe, California, at 0632Z (2232 PST) where a peak gust of 23 m/s (45 kts) was observed from the northeast. The outflow air continued to spread southward and wind speeds weakened (Figure 13). According to available data, after 0800Z (0000 PST, 11 August) the gust front became unidentifiable along a line from south of Phoenix to south of Yuma, Arizona, or approximately along the route of Interstate Highway 8.

Between 0100 and 0200Z (1700 and 1800 PST), the gust front moved out ahead of the MCC cloud visible in the satellite imagery (Figure 18). This separation appears to have occurred as the MCC reached maximum intensity. Perhaps this phenomenon marks the beginning of the dissipation phase of an MCC.

An unofficial report of the storm appeared on the front page of the Kingman Daily Miner dated 11 August 1981. From this news report it appears that the gust front arrived in the Kingman Area at about 0230Z (1930 PST). This time is consistent with satellite and radar data. The strong surface winds were accompanied by blowing dust. A thunderstorm occurred approximately "2 hours" after the arrival of the gust front. The strong winds were reported to have "caused only minor damage" in the Kingman area.

Based on satellite imagery, radar data, and surface observations, hourly positions of the leading edge of the gust front are shown in Figure 13. This figure illustrates that the outflow from the MCC spread rapidly southward. It traveled a total distance of nearly 575 km in approximately 12 hr for an average speed of 48 km/hr (30 mph). In many places the strong surface winds were accompanied by dense blowing dust and sand (Figures 3, 13 and 14) that reduced surface visibilities to zero. For example, in Las Vegas the surface visibility at LAS was ≤3 mi (4.8 km) for 45 to 60 min.

## H. Station Pressure

A characteristic of intense thunderstorms is a pronounced pressure jump accompanying the arrival of cold outflow air. Large pressure jumps were detected at stations located near the path of the MCC. Figure 14 illustrates the hourly changes in the station pressure at seven weather stations affected by the storm. Maximum hourly pressure rises of 3 to 5 mb/hr were measured at LSV, PRC, BLH, and DRA (not shown). Although large, these pressure jumps are less than those reported by Hales (1975) who described an intense, long-lived thunderstorm system that moved westward across Arizona. Figure 14 shows that the strongest surface winds occurred at those stations experiencing the largest pressure rises. Barometers located at stations near the edge of the dissipating outflow air mass (FLG, PHX, YUM) detected very small pressure increases with the accompanying wind shift.

## I. Surface Moisture

Changes in the surface-level moisture field are illustrated clearly by comparing Figures 15 through 17. Figure 15 is an analysis of the observed surface dew-point temperatures for 1200Z (0400 PST), Figure 16 is for 1800Z (1000 PST) just prior to rapid cumulonimbus development, and Figure 17 is for 0000Z (1600 PST) just before the thunderstorm activity reached LAS, LSV, and DRA. Figures 15 and 16 show that at the surface the axis of maximum atmospheric

26
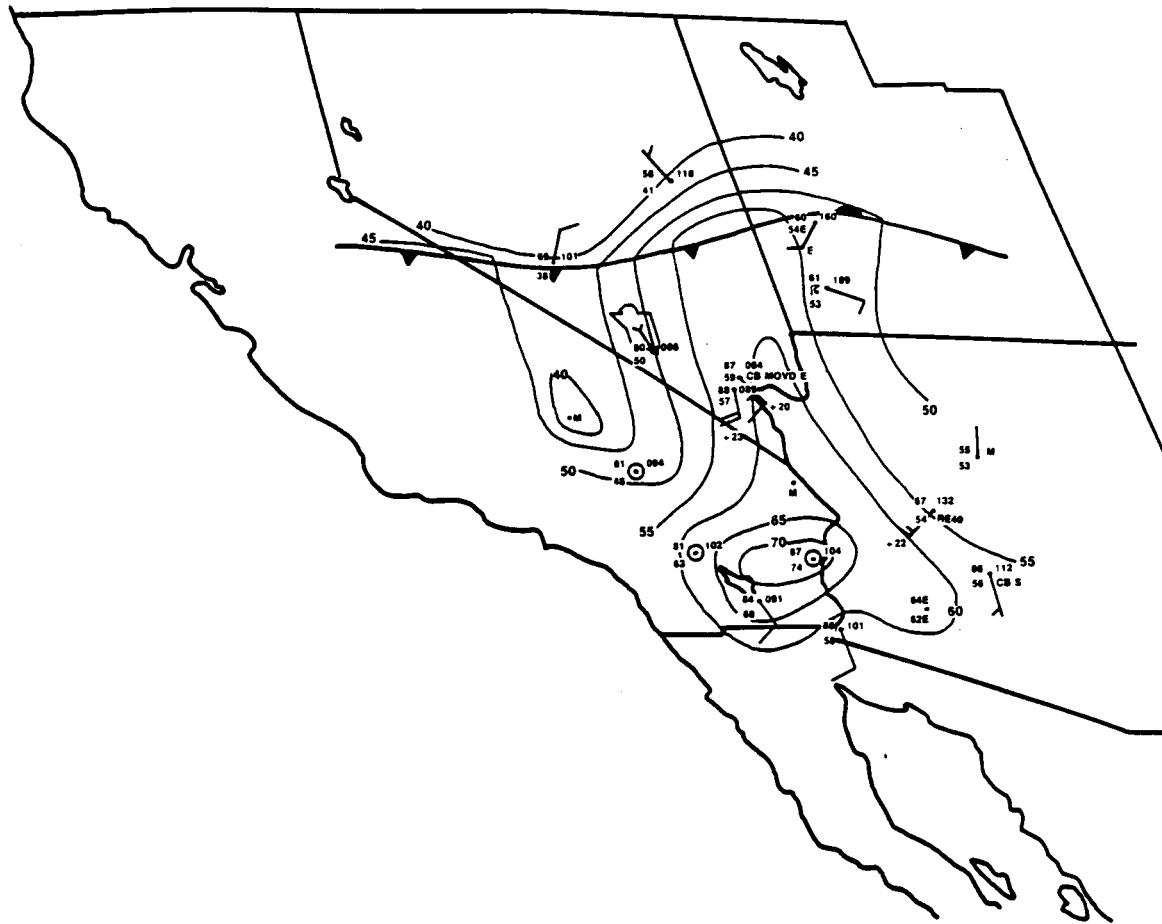
Figure 15. The 1200Z (0400 PST) analysis of surface dew-point temperature (°F) for 10 August 1981. Surface data and the frontal position are both plotted in the standard format.

Figure 16.  The 1800Z (1000 PST) analysis of surface dew-point temperature (°F) for 10 August 1981.  Surface data and the frontal position are both plotted in the standard format.

Figure 17.  The 0000Z, 11 August 1981 (or 1600 PST, 10 August) analysis of
surface dew-point temperature (°F).  Surface data and the frontal
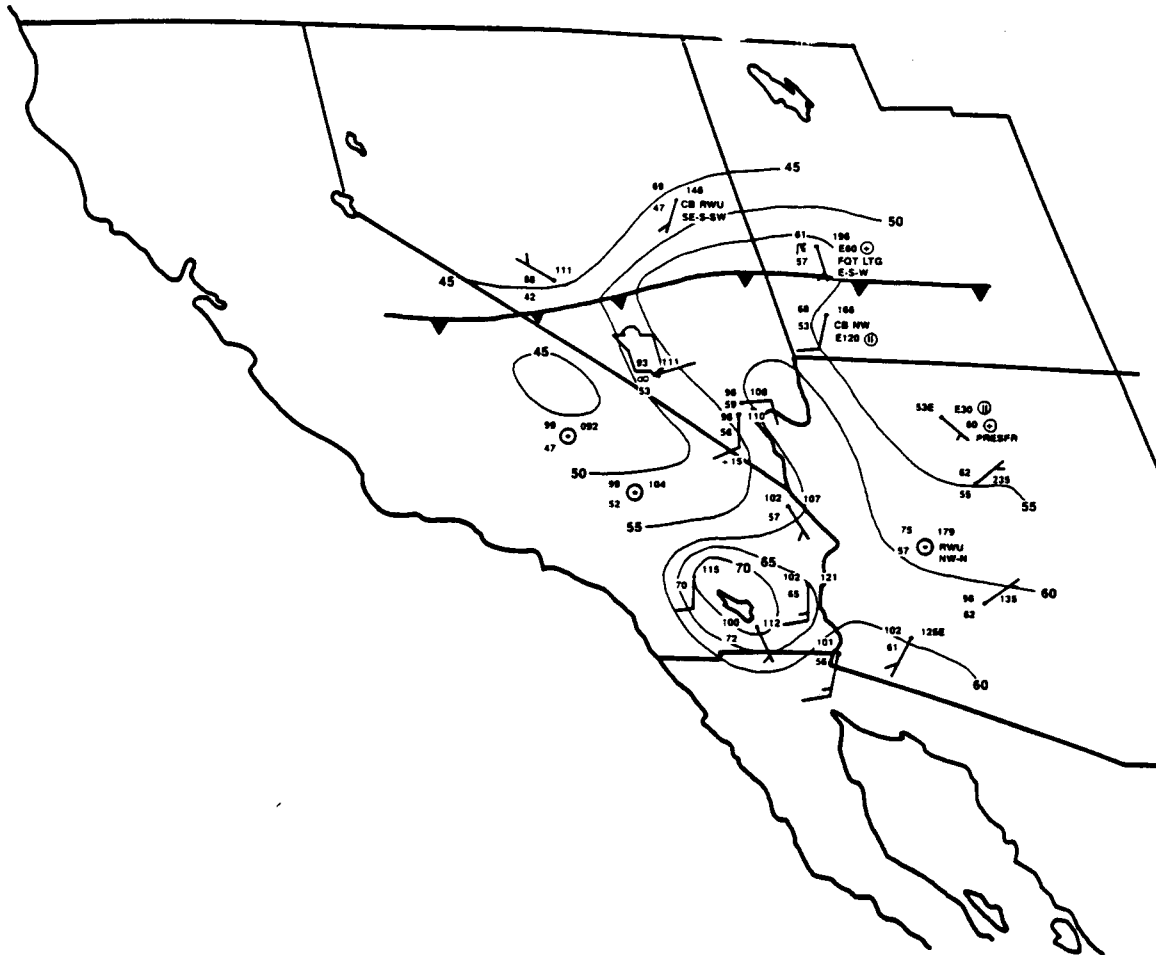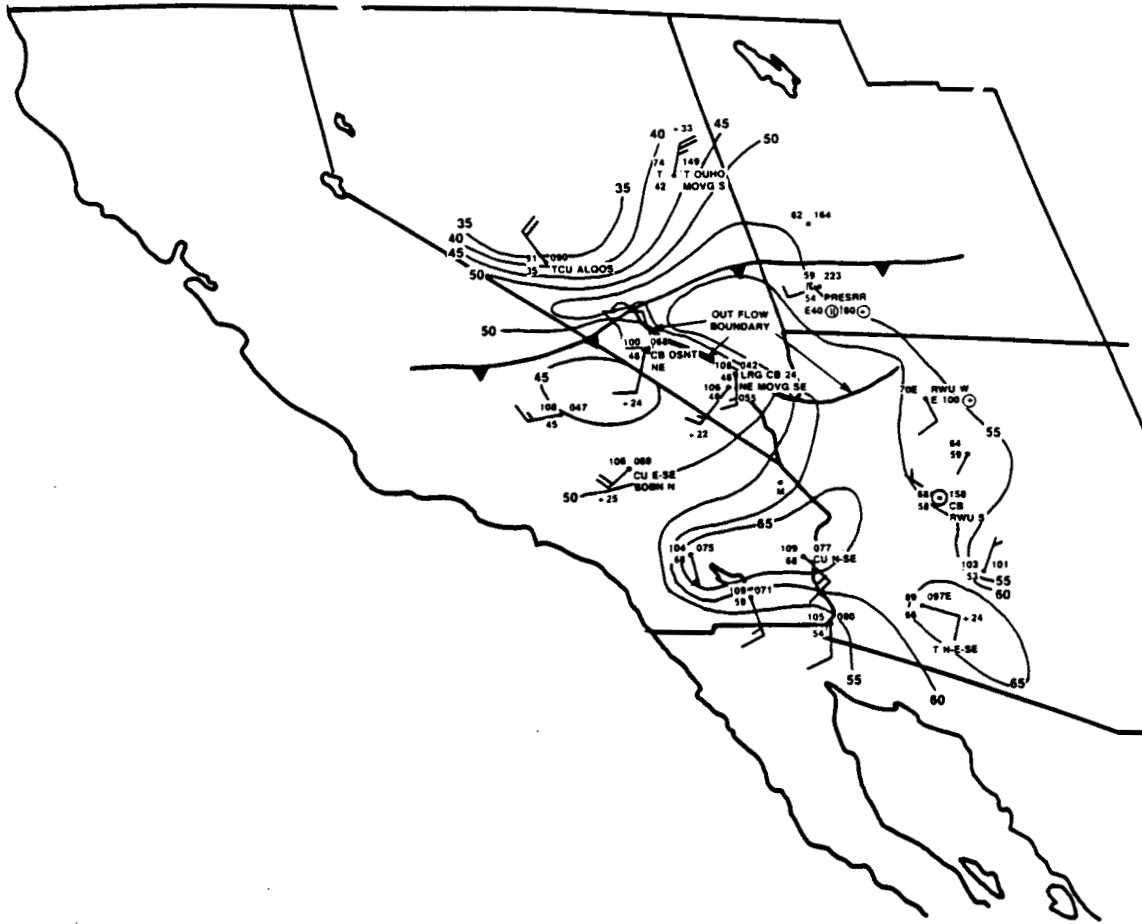position are both plotted in the standard format.  The leading edge
of the outflow from the MCC is also plotted in southern Nevada and
northwestern Arizona.

moisture content appeared to be slightly to the west of that at the 850-mb level (Figure 5) and extended northward across extreme southeastern Nevada. This position difference may be an artifact of the analyses since the data are not dense enough to provide high resolution of the three-dimensional structure of the moisture field. However, the available surface data show that in the Las Vegas valley the surface dew-point reached a maximum of 16°C (62°F) at 1400Z (0600 PST) at LSV while on the NTS it reached 12°C (55°F) at 1600Z (0800 PST) at DRA. Afterwards, surface dew-points decreased (Figure 17) to near 8°C (48°F) at LAS, LSV, and DRA just prior to the arrival of the strong surface outflow accompanying the MCC.

Mixing ratios associated with these changes in dew-point temperature were calculated. Prior to the drying that accompanied the southwesterly flow across southern Nevada, mixing ratios were 10 to 11 g/kg. With the development of southwesterly flow, mixing ratios decreased to 7 to 8 g/kg within about one hour. At 0000Z (1600 PST) the mixing ratio at LAS was 7.4 g/kg while 22.5 km northeast at LSV it was 10.7 g/kg for a mixing ratio gradient of 0.15 g/kg/km. Within one hour, from 0000Z to 0100Z (1600 to 1700 PST), the mixing ratio at LSV decreased by 3.5 g/kg, corresponding to a 10°F drop in dew-point temperature. More gradual changes were observed at DRA. With the arrival of the outflow from the MCC, mixing ratio values increased rapidly to 11 to 12 g/kg in precipitation.

Analyses of hourly surface data tend to show the development of a tight dew-point gradient across southern Nevada (Figures 15, 16, and 17). The role, if any, played by this tight gradient is not clear. However, the relationship between dry lines and severe thunderstorms has been recognized for many years (e.g., Beebe, 1958; Fujita, 1958; Henry and Thompson, 1963; Rhea, 1966; and others). Schaefer (1974) demonstrated that the boundary between dry and moist air can be nearly vertical above the ground but it is not clear if this type structure occurred with this storm.

The marked east-west gradient of elevated dew points across the NTS (Figure 17) is based on satellite and radar observations of convective clouds. Furthermore, the dew-point temperature at DRA decreased to 7°C (45°F) by 0100Z (1700 PST) and then increased to 17°C (62°F) by 0300Z (1900 PST) as the moist outflow from thunderstorms spread southward across the NTS. Thunderstorm activity began at DRA at 0130Z (1730 PST) and moved southeastward.

J. Surface Temperature

Pronounced temperature drops occurred at weather stations located under and near the MCC. For example, at LSV the temperature dropped from 42°C (108°F) at 0000Z (1600 PST) to 26°C (79°F) at 0100Z (1700 PST). Shortly after the rain began, the temperature dropped to 24°C (75°F) at 0255Z (1855 PST) for a total temperature decrease of 18°C (33°F). At LAS the temperature fell from 42°C (107°F) just prior to the arrival of the gust front to 28°C (83°F) one hour later, to 22°C (72°F) at 0350Z (1950 PST) after it started raining at 0301Z (1901 PST). Therefore, at LAS, the total cooling caused by the outflow was 20°C (35°F). At PRC the temperature fell from 22°C (72°F), 3 hours before the arrival of the gust front, to 14°C (58°F) at 0400Z (2000 PST) in a moderate thunderstorm. The gust front arrived at BLH at 0632Z (2232 PST). Between 0555Z (2155 PST) and 0647Z (2247 PST) the temperature dropped 6°C (10°F). At DRA the

temperature decreased from a maximum of 39°C (103°F) prior to thunderstorm
activity to 28°C (83°F) during a thunderstorm. A minimum temperature of 23°C
(74°F) was observed during thunderstorm activity at DRA. Figure 14 demonstrates
that these sharp temperature falls were accompanied by marked rises in surface
pressure.

Randerson (1982) and others have related thunderstorm-induced surface-
temperatu.e falls to the maximum observed speed of the surface wind gust from
the outflow. Pronounced temperature falls such as those observed at LSV and LAS
have been associated with outflow wind speeds of 26 to 36 m/s (50 to 70 kts).
Peak wind gusts observed and estimated to have occurred with the MCC fell within
this range.

K.  Satellite and Radar Data

Satellite and radar plots are displayed separately in Figure 18. The
satellite data make up the top half of Figure 18 and include some total rainfall
amounts which are listed in the left-hand margin (see Appendix B for city name
codes). The radar analysis is in the bottom half of the figure. In general,
both data sets were produced once an hour on the half hour. After 0415Z
(2015 PST) the IR satellite imagery was available at half-hour intervals. The
temporal and spatial evolution of the central part of the storm is summarized by
the analysis in Figure 18. This figure was constructed by first identifying the
path of the center of the storm across the ground. Then, the width of the storm
cloud was noted for times corresponding to satellite and radar data collection
times. This procedure was accomplished by plotting the storm track line on each
satellite or radar picture, overlaying the time line onto the newly plotted
storm track line, and marking the storm cloud boundaries and physical charac-
teristics onto the corresponding time line. This procedure was repeated for all
the available satellite and radar data. The plotted data were then analyzed,
producing the patterns shown in Figure 18. Pertinent surface observations and
radar intensity information were added along the appropriate time lines.

Detailed analyses of the infrared imagery of the storm cloud-top
temperatures showed that the coldest black body temperatures occurred between
2300 and 0500Z (1500 and 2100 PST). Cloud-top temperatures of -63 to -65°F
occurred over and near stations that reported the heaviest rainfall (see
Figure 20). Because of the poor resolution of the satellite imagery, it could
not be determined if "overshooting" occurred along the top of the storm cloud.

The radar data indicated significant thunderstorm activity occurred within
the storm cloud. Available radar charts are included in Appendix A. By 1935Z
(1135 PST), a very heavy (TRW++) thunderstorm was indicated to the south of Ely.
By 2035Z (1235 PST), very heavy thunderstorms had developed in this evolving
storm system. At 2035Z (1235 PST) a cloud top of 46,000 ft was reported by
radar observers. Very heavy to intense thunderstorm (TRWX) activity was
detected between 2035 and 0135Z (1235 and 1735 PST) in southern Nevada. Later,
at both 0235 and 0335Z (1835 and 1935 PST), radar reports indicated extreme
(TRWXX) thunderstorm activity over northwestern Arizona.

A comparison of the satellite and radar analyses in Figure 18 illustrates
several important points. The most intense radar echoes appear to lie along or
just ahead of the axis of coldest cloud tops. The area of heaviest rainfall
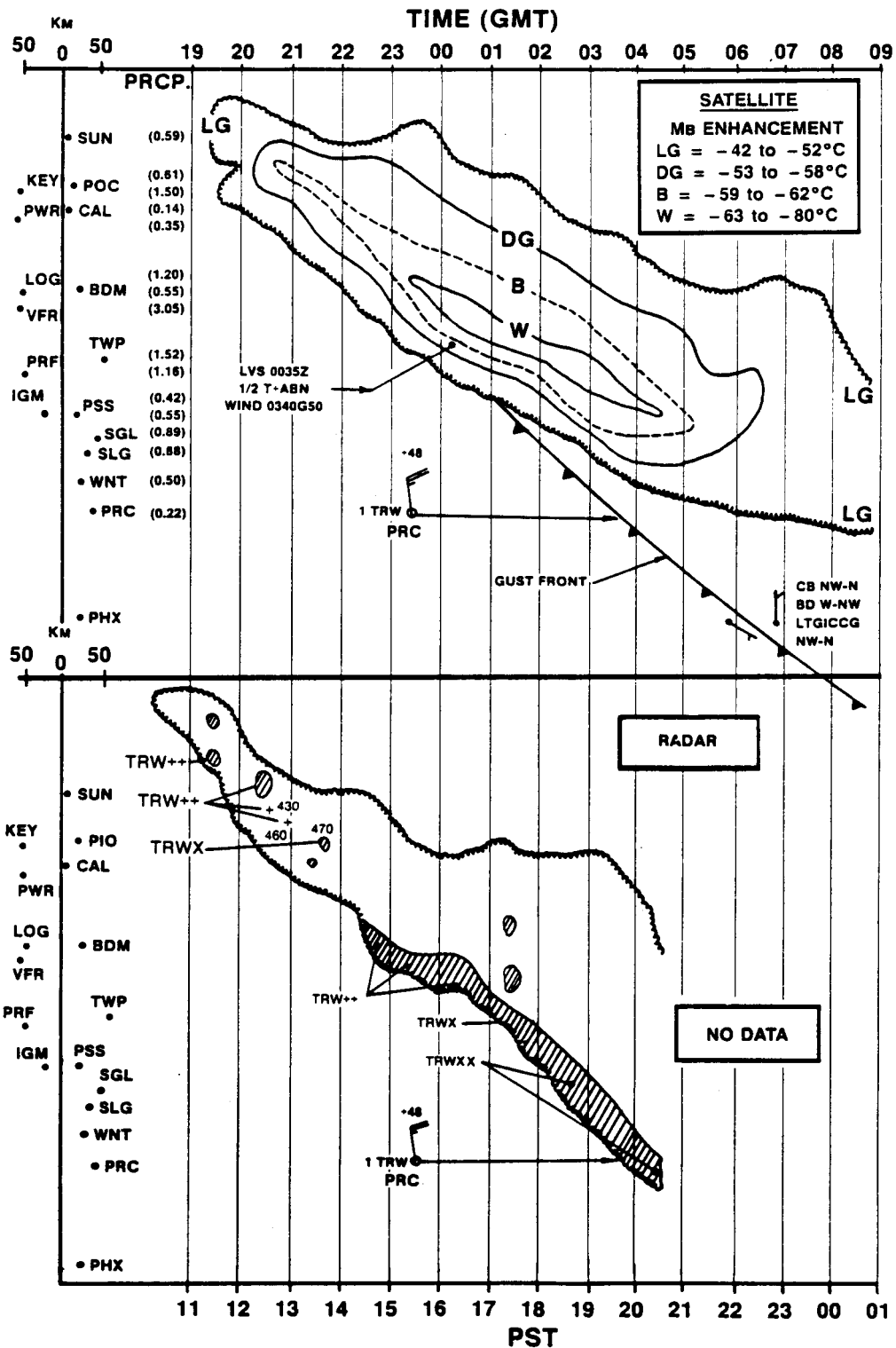appears to be under, or very near, the coldest cloud tops.

Figure 18. Composite of the time changes in the cloud-top temperatures (top) and radar echoes (bottom) along the track of the MCC. Total precipitation amounts in inches are plotted for stations located along the storm track (top left margin). The length scale represents distance east or west of the storm track for the locations of the precipitation data.

L.  Precipitation

Precipitation data were extracted from the August 1981 climatological data
booklets for Arizona, California, Nevada, and Utah.  These data are tabulated in
Appendix B.  Supplemental data came from a bucket survey conducted by the U.S.
Geological Survey (Glancy, 1981) for southern Nevada.  These bucket survey data
are listed in Table 3.

An isohyetal analysis of the total precipitation pattern resulting from the
storm of 10 August 1981 is shown in Figure 19.  For consistency, the analytical
results are presented on a satellite-map background, thereby facilitating the
ease of comparison between satellite and precipitation data.  Some of the rain-
fall was not caused by the MCC.  For example, the large area enclosed in the
one-inch contour in southwestern Utah, and the small maximum in central Arizona,
were both contaminated by thunderstorm rainfall from early in the day.  However,
the analyzed field over southern Nevada and northwestern Arizona was due to

Table 3.    Bucket Survey Precipitation Data for August 10, 1981*

| Site Letter (See Fig. 22) | Container Description | Precipitation in | (mm) |
|---|---|---|---|
| A | 52-cm diameter vertically standing can | 1.4 | ( 36) |
| B | 52-cm diameter vertically standing can | 0.7 | ( 18) |
| C | 15-cm diameter vertically standing can | 1.3 | ( 33) |
| D | Average of 8 vertically standing cans | 0.7 | ( 18) |
| E | 6.7-cm vertically standing cup | 1.9 | ( 48) |
| F | Standard rain gauge; Valley of Fire State Park | 3.0 | ( 76) |
| G | 9.8-cm vertically standing cans | 4.0 | (102) |
| H | 12.2-cm vertically standing can | 3.0 | ( 76) |
| I | 7.9-cm vertically standing glass jar | 1.9 | ( 48) |
| J | Distinct high-water line in vertically standing 5-gallon can.  Top of can was squashed, suggesting that the catch area was reduced. | 6.5 | (165) |
| K | Logandale University Experiment Station | 1.2 | ( 30) |

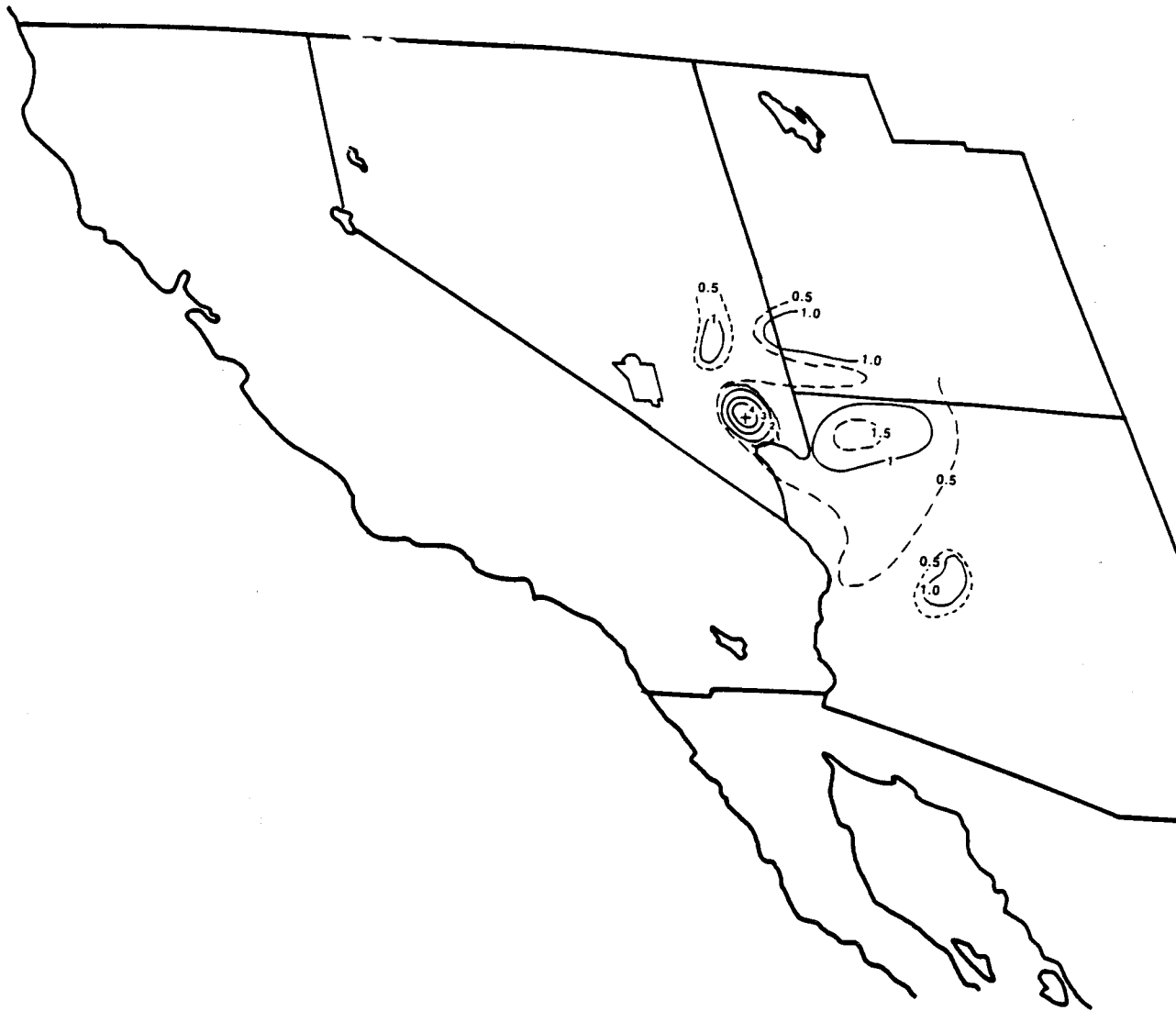*  Data provided by Pat Glancy, USGS, Carson City, NV.

Figure 19.  Analysis of the total precipitation in inches for 10 August 1981 in the vicinity of the MCC.  To convert from inches to millimeters, multiply inches by 25.4.

the MCC. Figure 19 shows that rainfall amounts in excess of 1 in (25.4 mm) accompanied the storm. The area enclosed within this one inch contour is approximately 25,000 $km^2$. Figure 20 helps to demonstrate that this area corresponds nicely with the occurrence of very cold cloud-top temperatures. The large precipitation area shown in Figure 19 (and detailed in Figure 22) is approximately 50 times larger than the one generated by the heavy thunderstorms that occurred over Las Vegas on 3 July, 1975 (Randerson, 1976a).

One area of extremely heavy rainfall was identified. This area is enclosed within the three-inch isohyetal contour in Figures 19 and 20. Identification of this area was substantiated by extensive property damage due to flooding in the Moapa/Overton area and to the disruption of vehicle traffic on Interstate Highway 15 (see Figure 21 for geographic locations). Quantitative estimates of the spatial distribution and total point rainfall amounts within this area are based on bucket survey data, on interviews with local residents, on a survey of the occurrence of streamflow in the normally dry washes, and on an assessment of property damage. Based on all the available information, it appears that 3 to 6 in (75 to 150 mm) of precipitation could have fallen to the southwest of the Logandale/Glendale area.

Field surveys conducted after the storm indicated that torrential rain probably fell around Ute, Nevada, and over the Valley of Fire State Park (Figure 21). Severe flooding occurred in these areas with water flowing over several miles of Interstate 15. Most of this rainwater flowed north and east into the Muddy River. The heavy rain that fell on the Valley of Fire State Park flowed eastward through Overton, Nevada, and east-southeastward into Lake Mead. Overton suffered extensive flood damage to homes and businesses. Farms along the Muddy River between Moapa and Overton suffered heavy flood damage and loss of livestock. Approximately 500 cows died in the flood waters (National Weather Service, 1981). Bucket-survey data collected by the USGS indicated that as much as 6 in (152 mm) of rain may have fallen near Ute. This survey is believed to be reliable because it had not rained in the area of interest since mid July. One properly exposed rain gauge was located within the area of heavy rainfall at the Valley of Fire State Park. A total of 3.05 in (77.5 mm) was collected in this gauge, but a small amount of the rainwater was spilled in the measurement process. Consequently, slightly more than 3.05 in actually fell. An isohyetal analysis of the estimated distribution of the heavy rain is given in Figure 22. The isohyetal pattern has an elliptical shape with the major axis oriented northwest-southeast. Thus, the axis of heaviest rainfall was oriented parallel to the storm track.

Hail was observed along the storm track across southern Nevada. The only official report of hail was from LSV, located northeast of downtown Las Vegas. At 0035Z (1635 PST), LSV reported a severe (T+) thunderstorm with hail one-fourth inch in diameter, visibility zero in blowing sand, and surface wind gusts of 58 kts (30 m/s). Larger hail, estimated to be 1 to 3 in (25 to 76 mm) in diameter was reported by residents in the Glendale area. Some of these individuals reported "large styrofoam-type balls floating in the flood water." Approximately 12 km southwest of Glendale, near Ute, desert yucca plants (Spanish Daggers) were damaged by large hail (Figure 23). These plants are rugged and can withstand considerable abuse; consequently, the breaking of their spears is thought to be significant and is believed to have been caused by large hailstones.

2246Z

2346Z

GLENDALE

LVS

TOTAL
RAINFALL
(INCHES)

0.5
0.5
1.0
1.0
1.5
1
0.5

ENHANCEMENT SCALE
(MB, 1981)

4: −32.2 to −41.2°C
5: −42.2 to −52.2°C
6: −53.2 to −58.2°C
7: −59.2 to −62.2°C
8: −63.2 to −80.2°C
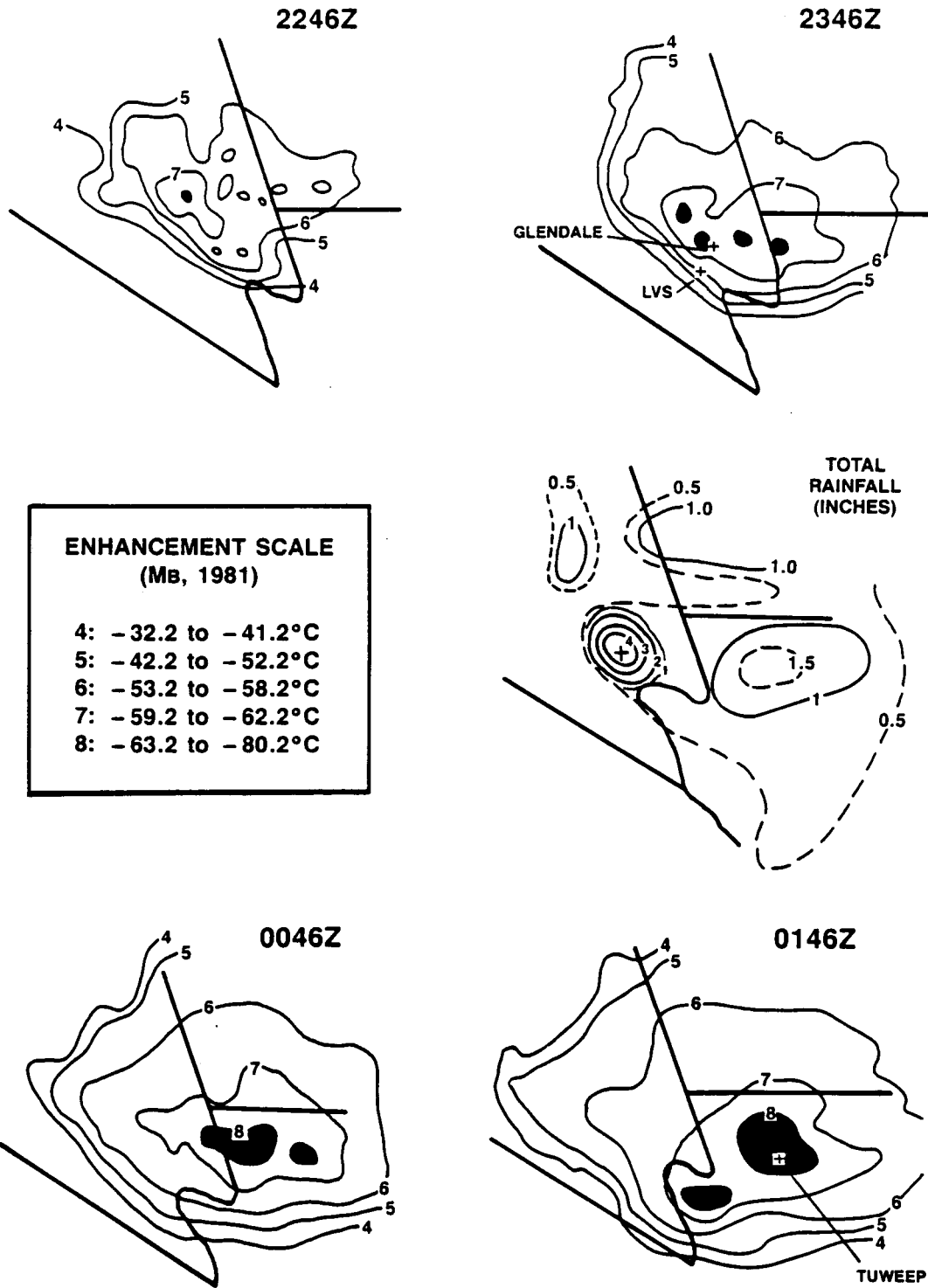
0046Z

0146Z

TUWEEP

Figure 20.   Composite of hourly satellite Infrared temperature measurements for
the period of the most Intense surface weather conditions.  The
total precipitation analysis from Figure 19 Is reproduced In the
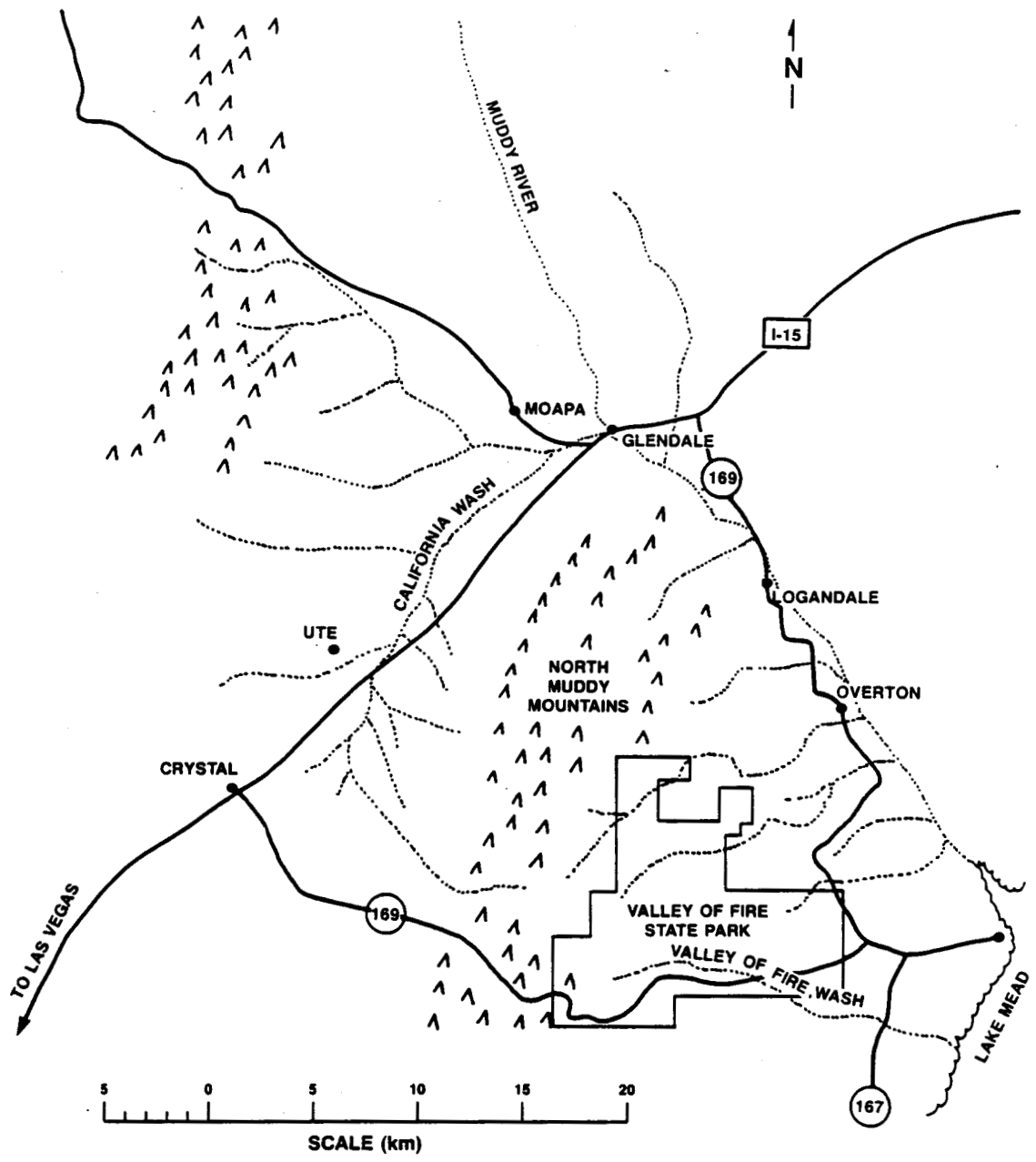middle for easy reference.

36

Figure 21.    Geographical locations of key points of interest for the flooding produced by the heavy rainfall generated by the MCC of 10 August 1981.
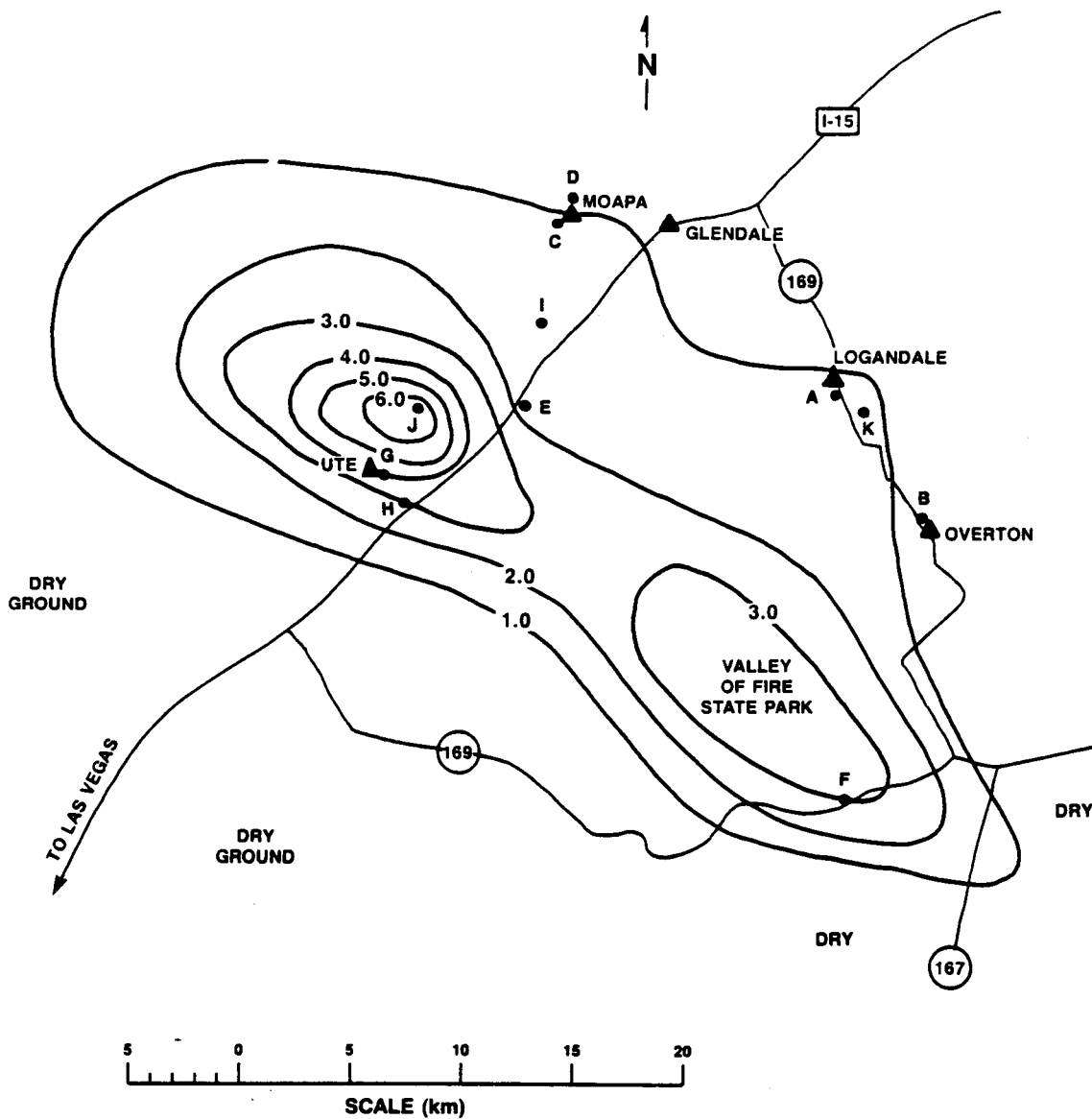
Figure 22.   Isohyetal analysis of the total precipitation pattern produced by
the intense rainfall from the MCC of 10 August 1981. The background
for this figure is that in Figure 21. Contours are in inches.
Station letters correspond to the bucket survey site letters
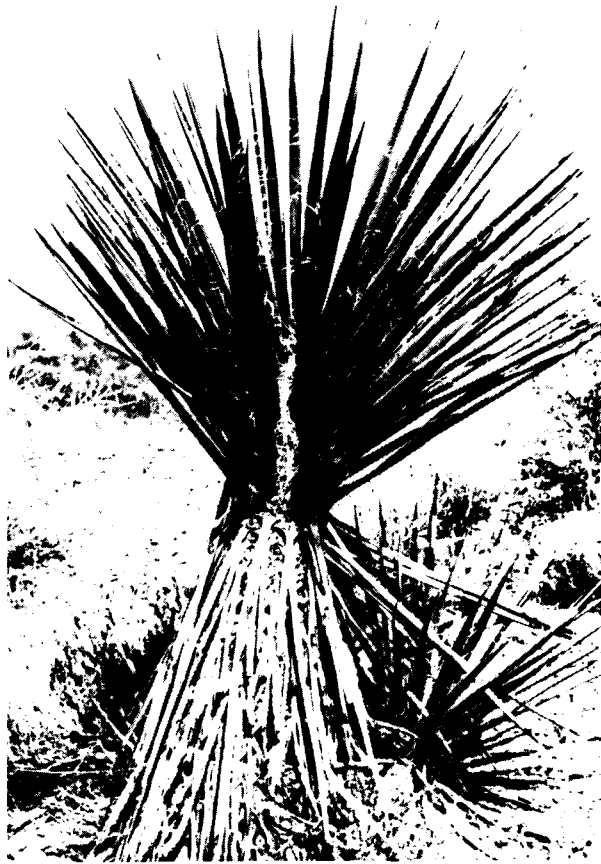tabulated in Table 3.

Figure 23.   Comparative photographs of a damaged (top) and undamaged (bottom) Spanish Dagger plant located in the area of large hail near Ute, Nevada (Figure 21).

39

Confidence in the distribution and intensity of the rainfall amounts is
relatively high. The areal coverage of the heavy ($\geq 1.0$ in) precipitation is
believed to be well formed. Not only was a bucket survey conducted to define
rainfall amounts, but also an assessment was made of the condition of the soil
and of numerous dry washes in the area of interest. Remember, no rain had
fallen in this area since mid July. Outside of the one-inch contour in
Figure 22, little or no stream flow was noted and the ground was observed to be
relatively dry with a lack of marked rill cuts in the soil. In addition, there
were no muddy areas where water had puddled. Considerable soil and vegetation
damage was identified within the one-inch contour. A large area to the east of
Glendale and to the north of the Colorado River was surveyed for additional
heavy flooding. No signs of flooding were found; however, this area is sparsely
populated and difficult to access. Consequently, it is not known with certainty
if any other areas of very heavy ($\geq 3.0$ in) rain occurred elsewhere. The
climatological data for northwestern Arizona did contain a rainfall total of
1.52 in (38.6 mm) at Tuweep. This station was located under a very cold cloud
top at 0146Z (1746 PST, Figures 9 and 20).

Rainfall rates with this storm were difficult to determine quantitatively
because of the lack of recording rain gauges. However, one station, the Logan-
dale University Experiment Farm, located on the eastern edge of the heaviest
rainfall, had a recording rain gauge. Data from this station indicated a rain-
fall rate of 0.8 in (20 mm) of rain in 15 min (3.2 in/hr) between 0045 and 0100Z
(1645 and 1700 PST). A total rainfall of 1.2 in (30.5 mm) was measured at this
station. This rainfall rate is consistent with that estimated for the storm.

The isohyetal field in Figure 22 was planimetered to obtain an estimate of
the total volume of water deposited on the ground and available for flooding
before infiltration. Within the 1.0 in (2.54 cm) contour, the total volume of
water was approximately $5 \times 10^8 m^3$ ($4 \times 10^5$ acre ft). To compare the rainfall
volume of this storm with the Las Vegas storm of 3 July, 1975 (Randerson,
1976a), the position of the 0.5-in contour had to be estimated. For this
purpose, the 0.5-in contour was assumed to be concentric with the 1.0-in contour
and to have a gradient equivalent to that between the 1.0 and 2.0 in isohyets.
Planimetry showed that within the 0.5-in contour the total volume of water was
approximately $7 \times 10^8 m^3$ ($6 \times 10^5$ acre ft), or, roughly $10^9 m^3$ within the pre-
cision of the data and the isohyetal analysis. In the Las Vegas storm of
3 July, 1975, similar calculations showed that $2.3 \times 10^7 m^3$ ($1.9 \times 10^4$ acre ft)
of water were available to the natural drainage channels in a period of 2 to
4 hr (Randerson, 1976a). Consequently, based on the volume of rainfall water
produced, the storm of 10 August 1981, was 30 times larger than the 1975 storm.
Within the half-inch contour, the intense rainfall in the Ute area produced
approximately $5 \times 10^8 m^3$ ($4 \times 10^5$ acre ft) of water while roughly $2 \times 10^8 m^3$
($1.6 \times 10^5$ acre ft) fell in the vicinity of the Valley of Fire State Park.

M.  Streamflow

According to calculations and measurements made by the USGS (Glancy, 1981),
streamflow rates of 5,000 to 10,000 ft³/s (142 to 283 m³/s) occurred in many of
the dry washes to the southwest of the Logandale/Glendale area. Extensive
flooding occurred along the California Wash and in the vicinity of Ute. A maxi-
mum stream flow rate of about 50,000 ft³/s (1,557 m³/s) was estimated to have
occurred on the California Wash to the south of Moapa (Glancy, 1981). Flood
waters 2 to 4 ft (0.6 to 1.2 m) deep were reported to have covered Interstate 15

where California Wash crosses the highway (Figure 21). To the south of Glendale, in the Valley of Fire Wash (Figure 21), a streamflow rate of about 20,000 ft$^3$/s (566 m$^3$/s) was calculated where the wash flowed under Nevada State Highway 167. At this point a culvert was completely destroyed. Along the same stream, the culverts on Nevada State Highway 169, in the Valley of Fire State Park, were also totally destroyed. The USGS is assembling a separate report on this storm. According to the National Weather Service (1981) "the flooding and high wind caused 10's of millions of dollars worth of damage to the Moapa area, Lake Mead Recreation Area, and Las Vegas."

Flooding was reported to the west of Kingman, Arizona, in the <u>Kingman Daily Miner</u>. The newspaper reported that Arizona Highway 68 was closed due to flooding in the Sacramento and Twin Washes.

N. Dissipation

As the MCC continued moving southeastward, cloud tops began to warm after 0400Z (2000 PST). Figures 24 and 25 clearly demonstrate this thermal change. In addition, the outflow winds from the storm system began to move out ahead of the MCC cloud mass between 0100 and 0200Z (1700 and 1800 PST). The accompanying gust front can be easily identified in Figures 24 and 25. As it moved out ahead of the MCC, the gust front did not appear to initiate any significant new convection. The gust front was identifiable in the satellite imagery from 0446Z (2046 PST) until nearly 0900Z (0100 PST). It appears that as the outflow from the MCC began to move away from the MCC, the MCC began to dissipate. Debris clouds from the MCC were identifiable on satellite imagery until approximately 1500Z (0700 PST) on 11 August.

### III. CONCLUSIONS

A large, long-lived, mesoscale convective weather system developed over east central Nevada on 10 August 1981. This storm system satisfied many of the criteria associated with Mesoscale Convective Complexes (Maddox, 1980). These criteria are rigid. Consequently, with some flexibility, an analysis of all available meteorological data in conjunction with satellite imagery and radar data indicate that this storm qualified for a β mesoscale (Orlanski, 1975) system or an MCC. The only MCC characteristic not met was duration criteria B (Maddox, 1980) which was met for only 5 hr not $\geq$6 hr.

MCC development occurred ahead of a southeastwardly moving short-wave trough. Rapid development took place in the early afternoon as an upper tropospheric jet of westerly winds ahead of the trough moved over low-level warm, moist air covering extreme southeastern Nevada. As the MCC generated it moved south-southeastward at an average speed of 40 km/hr (25 mph). Strong convergence occurred on the right flank (west side) of the MCC and along a tight moisture gradient located slightly northeast of Las Vegas. Strong mass convergence developed along this tight gradient where relatively dry southwesterly flow of 5 to 10 m/s met strong (20 to 30 m/s) and relatively cold northeasterly outflow air from the MCC. Very cold cloud tops ($T_{bb}$ =-65°C) developed and intense rain fell to the northeast of this strong convergence zone.

Based on the 0000Z (1600 PST) winds-aloft data (see Table 2) and on the assumption that cloud bases in the MCC were at or near the 10,000-ft level
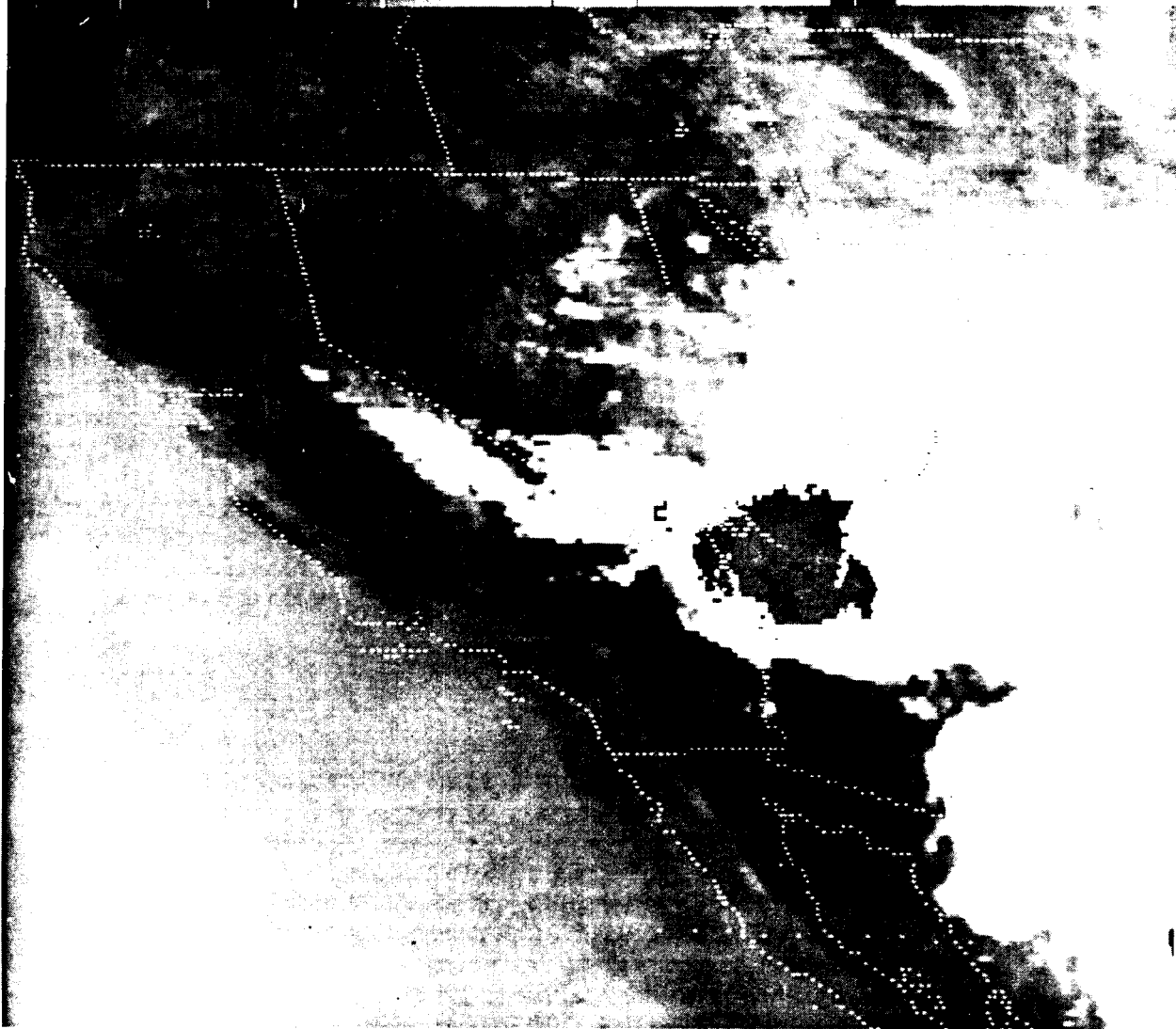
Figure 24.   Infrared satellite imagery with MB enhancement for 0446Z,
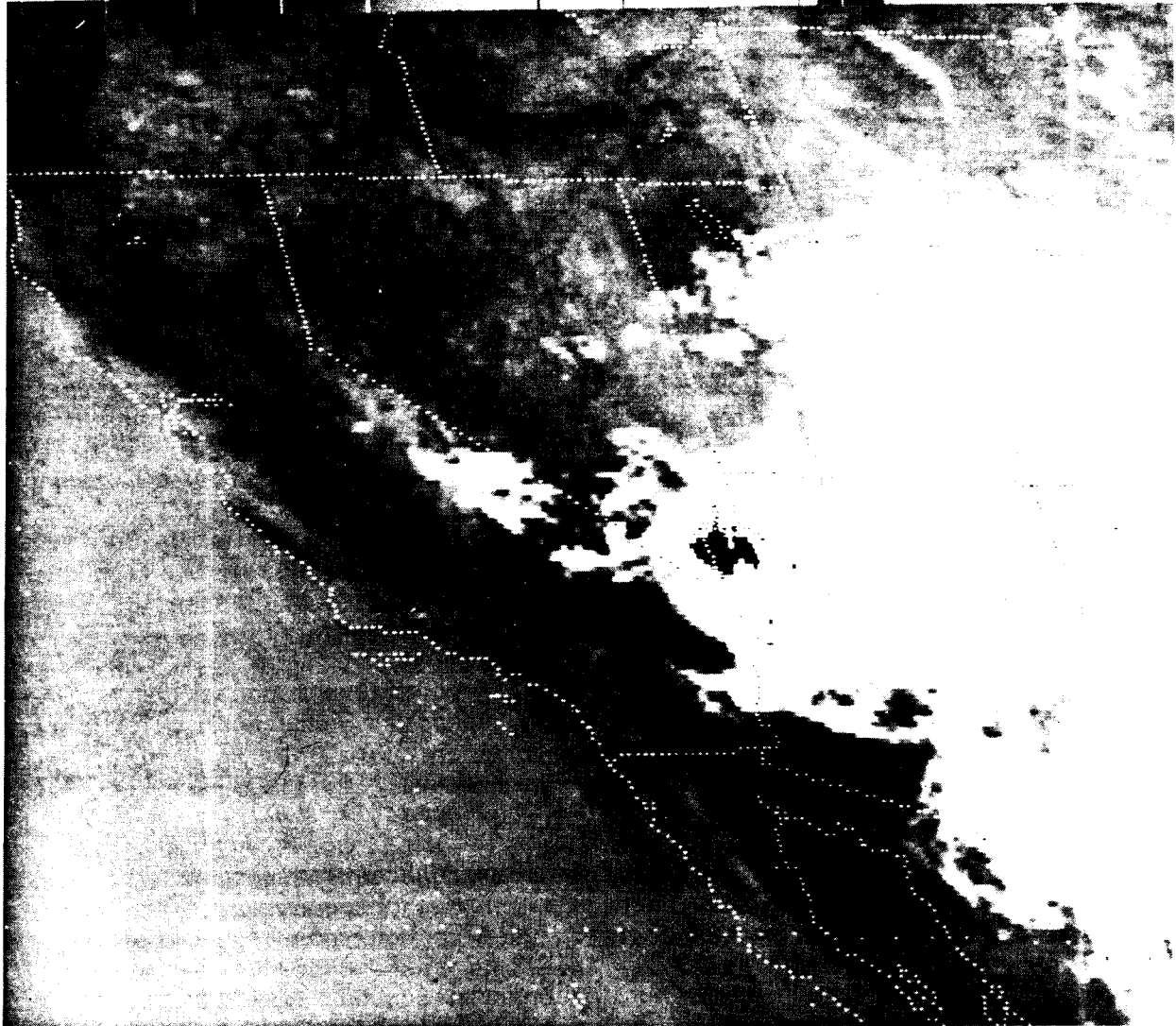11 August 1981, or 2046 PST, 10 August.

Figure 25.   Infrared satellite imagery with MB enhancement for 0646Z,
11 August 1981, or 2246 PST, 10 August.

43

above mean sea level, the following conclusions were made:

1.  Below the cloud bases the mean inflow wind was from 215° at 10 m/s with essentially no direction or speed shear in the vertical.

2.  Mean environmental cloud-layer winds were from 300° at 12 m/s with very little direction or speed shear through the layer.

3.  Storm movement was from 345° at 15 m/s or 45° to the right of the direction of the mean environmental cloud-layer winds.

4.  Sub-cloud layer air therefore had a strong component of relative motion toward the approaching storm. Consequently, a zone of strong enhancement of vertical motion existed along and to the right (west side) of the MCC. The coldest cloud tops and heaviest rainfall occurred along and to the east of this convergence zone.

Total rainfall amounts of 3 to 6 in (76 to 152 mm) occurred to the southwest of Glendale. As much as 6 to 6.5 in (152 to 165 mm) appears to have fallen near Ute, while 3.05 in (77.5 mm) fell in a rain gauge located in the Valley of Fire State Park. Rainfall rates were estimated to be 3 to 4 in/hr (76 to 102 mm/hr) or more. This intense rainfall caused extensive flooding in the Moapa area. Calculations made from field survey measurements by the USGS showed that many normally dry stream beds experienced streamflow rates of 5,000 to 10,000 ft³/s (142 to 283 m³/s). A maximum streamflow rate of about 50,000 ft³/s (1,560 m³/s) is estimated to have occurred near the mouth of the California Wash. Much property damage and loss of livestock was attributed to the flooding.

On the right flank of the MCC, strong surface outflow winds of 50 to 70 kts (26 to 36 m/s) caused property damage, power blackouts, and injuries from flying debris. Many boats were damaged by strong winds on Lake Mead. In addition, dense clouds of blowing dust and sand were generated, limiting visibility to less than 3 mi (4.8 km) for 45 to 60 min in Las Vegas.

MCC type storms have important societal consequences in the desert southwest. The accompanying heavy precipitation can cause devastating flash floods if the storm passes over a populated area. Much property damage and loss of life can occur (Randerson, 1976a). The strong surface winds can destroy buildings, cause flying debris, and raise dense clouds of blowing dust and sand, thereby reducing local visibilities to zero. Blowing dust and sand and strong winds are hazardous to airplanes, to boats, and to vehicular traffic. The strong winds, heavy rain, and cloud-to-ground lightning can disrupt electric power supplies in an area where many homes and businesses are "all electric".

The level of experience and awareness of the potential dangers of MCC type storms in the desert southwest may be low because many people have moved into this area recently. Upon seeing the desert conditions, some may erroneously assume that heavy rain, strong surface winds, flash flooding, and lightning don't occur often and are not serious problems. An educational program may be needed to raise awareness.

It is important to note that a very similar type storm developed north of Glendale on June 30, 1984 (Cylke, 1984). Locally heavy rain, blowing dust and

sand, and surface wind gusts of 25 to 30 m/s (50 to 60 kts) accompanied this storm. Maximum rainfall totals were probably 1.5 to 3.0 in (38 to 76 mm) in the Caliente/Pioche area. Rainfall totals in the Las Vegas Valley were in the 0.1 to 0.5 in (2.5 to 12.7 mm) range. Some street flooding did occur in Las Vegas and electric power supplies were disrupted.

The climatology of MCC type storms over the southwestern United States and northwestern Mexico is unknown. Based on personal review of satellite imagery of the the past 10 yr and on limited written documentation (Cylke, 1984 and Hales, 1975), it appears that these large, well organized thunderstorms may occur more frequently than expected over the southwestern United States. More complete documentation of these storms is needed by hydrologists who are assigned the task of designing flood control systems and by meteorologists who must forecast their occurrence and alert the general public.

## ACKNOWLEDGEMENTS

# REFERENCES

Bailey, H. P., 1966: _The Climate of Southern California_, University of California Press, Los Angeles, 87 pp.

Bartels, D. L., Skradski, J. M., and Menard, R. D., 1984: Mesoscale convective systems: A satellite-data-based climatology. _NOAA Technical Memorandum ERL ESG-8_, Boulder, CO, 58 pp.

Beebe, R. G., 1958: An instability line development as observed by the tornado research airplane. _J. Meteorol._, 15, 278-282.

Blake, D., 1923: Sonora storms. _Mon. Wea. Rev._, 51, 585-588.

Benner, H. P., 1965: Evaluation of the operational feasibility of utilizing ARTC radar at Salt Lake City for weather surveillance. Weather Bureau Western Region publication, 31 pp.

Brenner, I. A., 1974: A surge of maritime tropical air - Gulf of California to the southwestern United States. _Mon. Wea. Rev._, 102, 375-389.

Cylke, T., 1984: Mesoscale analysis of a flash flood producing thunderstorm complex in southern Nevada. _Western Region Technical Attachment No. 84-29_, Salt Lake City, Utah, 5 pp.

Fujita, T. T., 1978: _Manual of Downburst Identification for Project NIMROD_. Satellite and Mesometeorology Research Project, Dept. of Geophysical Sciences, University of Chicago, Chicago, IL, 104 pp.

_____, 1958: Structure and movement of a dry front. _Bull. Am. Meteorol. Soc._, 39, 574-582.

George, J. J., 1960: _Weather Forecasting for Aeronautics_, Academic Press, 673 pp.

Glancy, P. A., 1981: Personal Communication.

Grebe, R., 1982: An outline of severe local storms with the morphology of associated radar echoes. _NOAA Technical Memorandum NWSTC-1_, 80 pp.

Hales, J. E., 1975: A severe southwest desert thunderstorm: 19 August 1973. _Mon. Wea. Rev._, 103, 344-351.

_____, 1974: Southwestern United States summer monsoon source - Gulf of Mexico or Pacific Ocean? _J. Appl. Meteorol._, 13, 341-342.

_____, 1972: A study of radar echo distribution in Arizona during July and August. _NOAA Technical Memorandum NWSWR-77_, 21 pp.

Henry, W. K., and Thompson, A. H., 1963: The Texas dew-point front as seen by TIROS-1, Scientific Report No. 3. Texas A&M Research Foundation, College Station, Texas, 28 pp.

Idso, S. B., 1975: Arizona weather watchers: past and present. <u>Weatherwise</u>, <u>28</u>, 56-60.

_____, Ingram, R. S., and Pritchard, J. M., 1972: An American haboob. <u>Bull. Amer. Meteorol. Soc.</u>, <u>53</u>, 930-935.

Maddox, R. A., 1983: Large scale meteorological conditions associated with midlatitude, mesoscale convective complexes. <u>Mon. Wea. Rev.</u>, <u>111</u>, 1475-1493.

_____, 1980: Mesoscale convective complexes. <u>Bull. Amer. Meteorol. Soc.</u>, <u>61</u>, 1374-1387.

_____, 1976: An evaluation of tornado proximity wind and stability data. <u>Mon. Wea. Rev.</u>, <u>104</u>, 133-142.

National Weather Service, 1981: Report on the Moapa Valley flash flood August 10, 1981. Western Region Headquarters, Salt Lake City, UT, 23 pp.

Orlanski, I., 1975: A rational subdivision of scales for atmospheric processes. <u>Bull. Amer. Meteorol. Soc.</u>, <u>56</u>, 527-530.

Petterssen, S., 1956: <u>Weather Analysis and Forecasting</u>. McGraw-Hill Book Company, Inc., New York, 428 pp.

Randerson, D., 1984: <u>Atmospheric Science and Power Production</u>, DE84005177 (DOE/TIC-27601), National Technical Information Service, U.S. Dept. of Commerce, Springfield, VA, 850 pp.

_____, 1982: Approximations to the peak surface wind gusts from desert thunderstorms. <u>NOAA Technical Memorandum NWS WR-176</u>, National Weather Service Western Region, Salt Lake City, UT, 16 pp.

_____, 1977: Spatial variability of warm season echo activity as a function of two stability indices computed from the Yucca Flat, Nevada, radiosonde. <u>Mon. Wea. Rev.</u>, <u>105</u>, 1590-1593.

_____, 1976a: Meteorological analysis for the Las Vegas, Nevada, flood of 3 July, 1975. <u>Mon. Wea. Rev.</u>, <u>104</u>, 719-727.

_____, 1976b: Summertime radar echo distributions of moist convection over southern Nevada and adjacent areas for 1971 and 1972. <u>NOAA Technical Memorandum ERL ARL-58</u>, Air Resources Laboratory, Las Vegas, Nevada, 37 pp.

Reynolds, D. W., and Vonder Haar, T. H., 1979: Satellite support to HIPLEX: summary of results 1976-1978. Final report, Bureau of Reclamation Contract #6-07-DR-20020, Colorado State University, Ft. Collins, CO, 89 pp.

Rhea, J. O., 1966: A study of thunderstorm formation along dry lines. <u>J. Appl. Meteorol.</u>, <u>5</u>, 59-63.

Ronne, E. E., 1971: Precipitation detection probabilities by Los Angeles ARTC radars. <u>NOAA Technical Memorandum NWS WR67</u>, 14 pp.
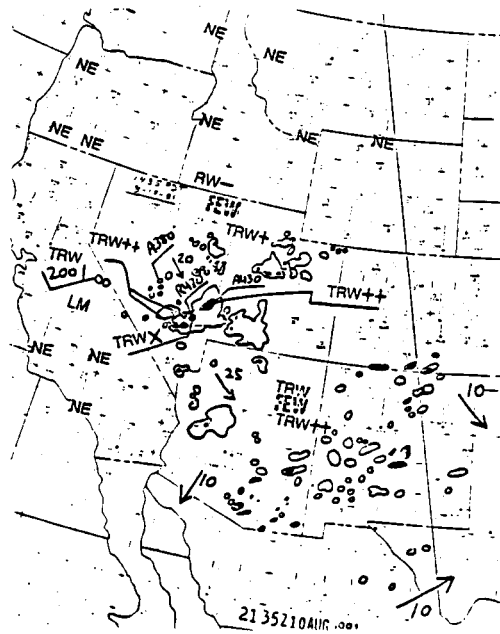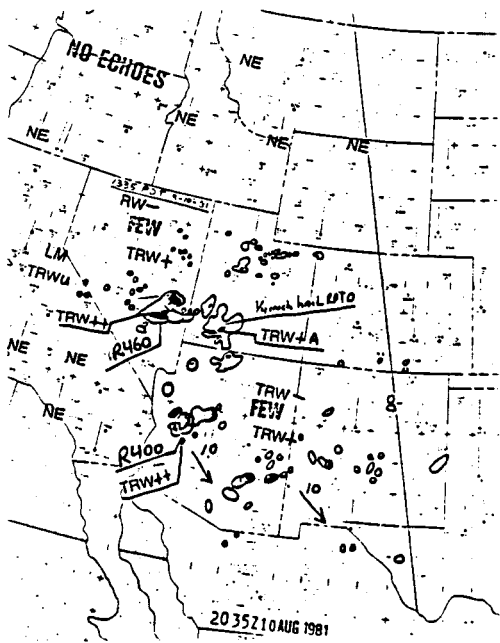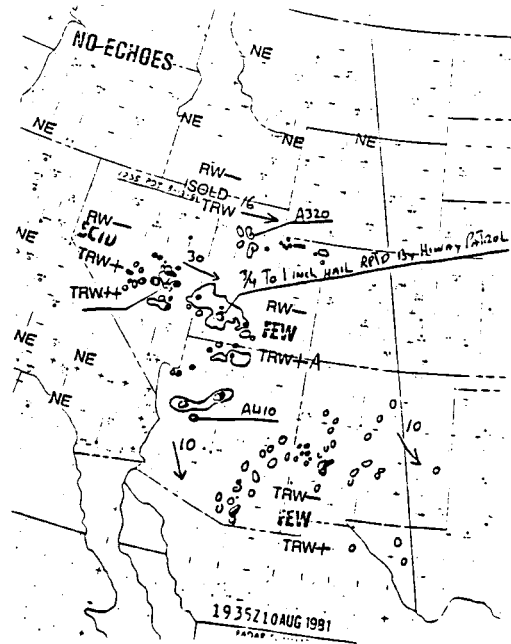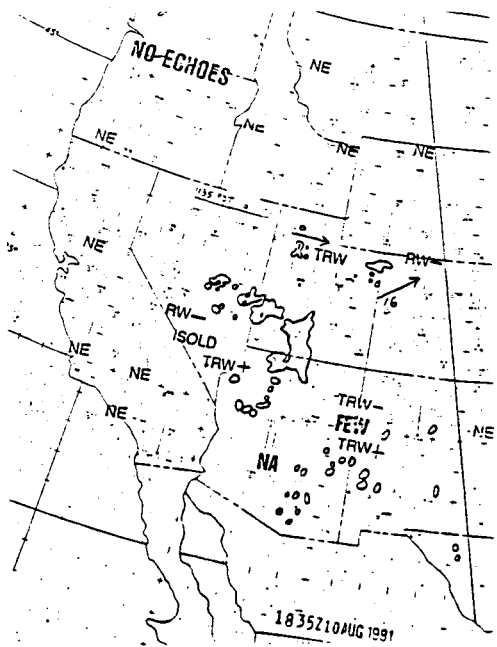
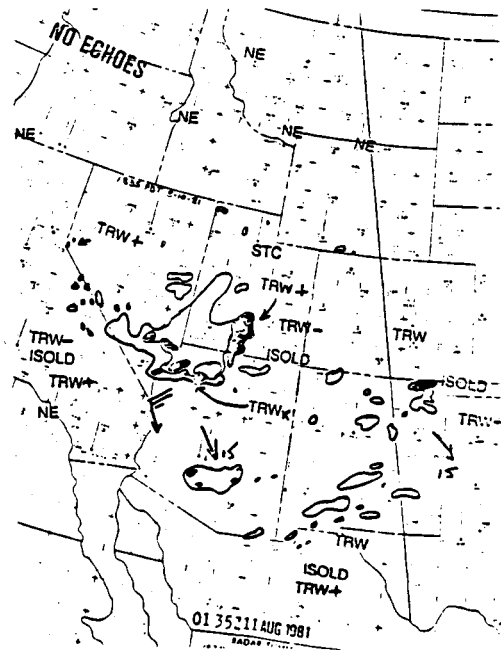Sakamoto, C. M., 1972: Thunderstorm and hail days probabilities in Nevada. NOAA Technical Memorandum NWS WR74, 25 pp.
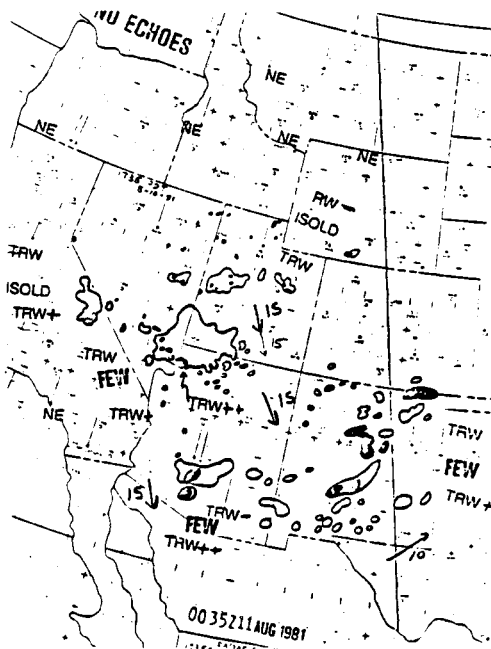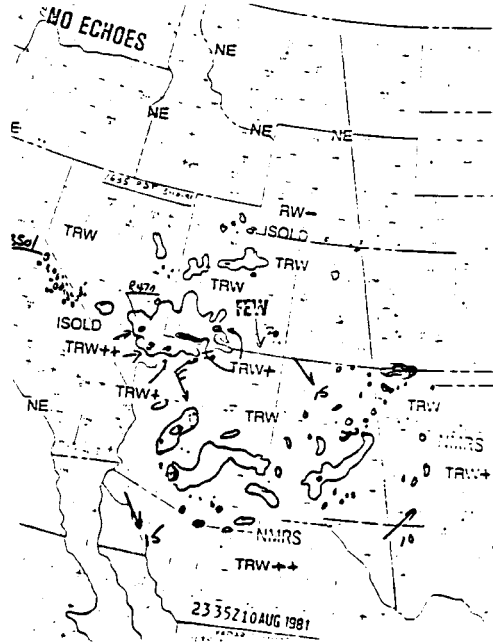
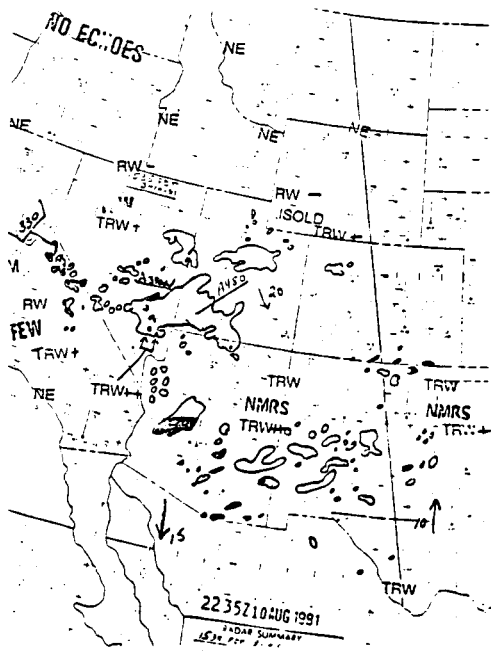Schaefer, J. T., 1974: The life cycle of the dryline. J. Appl. Meteorol., 13, 444-449.

Scofield, R. A., and Oliver, V. J., 1977: A scheme for estimating convective rainfall from satellite imagery. NOAA Technical Memorandum NESS 86, Washington, D.C., 47 pp.

Stackpole, J. D., 1967: Numerical analysis of atmospheric soundings, J. Appl. Meteorol., 6, 464-467.

APPENDIX A.  AIR ROUTE TRAFFIC CONTROL RADAR CHARTS FOR 10 AUGUST 1981

Total rainfall amounts in inches for August 10, 1981 from National Climatological Data Center Records for August 1981.  Data listing is chronological, from stations first experiencing the storm to the last.

| Approx. Time (GMT) | Nevada (Utah) | Map ID | Tot. Amt. Rain | Arizona | Map ID | Tot. Amt. Rain |
|---|---|---|---|---|---|---|
| 1800 | Sunnyside | SUN | 0.59 | | | |
| | Adaven | ADV | 0 | | | |
| | Lake Valley | | 0 | | | |
| | Spring Valley State Park | | 1.08 | | | |
| 1900 | Tempiute | | 0.07 | | | |
| | Pioche | POC | 0.61 | | | |
| | Key Pittman | KEY | 1.50 | | | |
| 2000 | Caliente | CAL | 0.14 | | | |
| | Modena, Utah | | 1.42 | | | |
| 2100 | Enterprise, Utah | | 0.80 | | | |
| | Pahranagut W.L. Refuge | PWR | 0.35 | | | |
| 2200 | Elgin | | 0 | | | |
| | Gunlock, Utah | | 0.32 | | | |
| 2300 | St. George, Utah | | 0.30 | Beaver Dam | BDM | 0.55 |
| | Logandale Un. Exp. Farm | LOG | 1.20 | Pipe Springs Nat. Mon. | | 1.57 |
| 0000 | Valley of Fire State Pk. | VFR | 3.05 | | | |
| | Sunrise Manor (Las Vegas) | | 0.14 | | | |
| 0100 | Las Vegas | LAS | 0.07 | | | |
| | Boulder City | | 0.23 | Willow Beach | | 0.98 |
| | | | | Pierce Ferry | PRF | 1.16 |
| | Searchlight | | 0.22 | Tuweep | TWP | 1.52 |
| | | | | Supai | | 1.34 |
| 0200 | | | | Bright Angel | RS | 0.83 |
| | | | | Grand Canyon Nat. Pk. | | 0.80 |
| 0300 | | | | Peach Springs | PSS | 0.55 |
| | | | | Bullhead City | | 0.38 |
| 0400 | | | | Kingman | IGM | 0.47 |
| | | | | Seligman | SEL | 0.89 |
| | | | | Seligman (13 mi SSW) | SLG | 0.80 |
| | | | | Lake Havasu | | 0.01 |
| | | | | Wikiup | | 0.71 |
| | | | | Walnut Creek | WNT | 0.50 |
| | | | | Chino Valley | | 0.11 |
| | | | | Alamo Dam | | 0.28 |
| | | | | Hillside (4 mi NNE) | | 0.47 |
| 0500 | | | | Jerome | | 1.72 |
| | | | | Prescott | PRC | 0.22 |
| | | | | Beaver Creek | | 0.39 |
| | | | | Walnut Grove | | 1.32 |
| 0600 | | | | Cordee | | 0.03 |